Netherlands Journal of Geosciences

Original Article

Cite this article: Jasper Maars et al. *Causes of uncertainty in geomodelling inputs: data review of Paleozoic geology in the Euregion Meuse-Rhine. Netherlands Journal of Geosciences*, Volume 105, e12991. https://doi.org/10.70712/NJG.v105.12991

Received: 16 July 2025
Revised: 13 January 2026
Accepted: 13 March 2026
Published: 18 May 2026

Keywords:
geological uncertainties; legacy data; boreholes; cartography; stratigraphy; data compilation

Corresponding author:
Jasper Maars,
Email: jasper.maars@tno.nl

Supplementary material
The supplementary material for this article can be found at https://doi.org/10.70712/NJG.v105.12991.

Causes of uncertainty in geomodelling inputs: data review of Paleozoic geology in the Euregion Meuse-Rhine

Jasper Maars[1,2], Jasper Hupkes[1], Alexander J.P. Houben[2], Geert-Jan Vis[2], Allard W. Martinius[1,3], Cornelis R. Geel[2], Marleen De Ceukelaire[4], Hemmo A. Abels[1]

[1]Department of Geoscience and Engineering, Delft University of Technology, Stevinweg 1, 2628 CN, Delft, The Netherlands; [2]TNO – Geological Survey of the Netherlands, Princetonlaan 6, 3584 CB Utrecht, The Netherlands; [3]Equinor ASA, Arkitekt Ebbellsvei 10, Trondheim, Norway; [4]Royal Belgian Institute of Natural Sciences—Geological Survey of Belgium, Jennerstraat 13, 1000 Brussels, Belgium

Key points

- Sources of uncertainty in geomodelling inputs are identified and categorised.
- A subsurface dataset is compiled, and data inconsistencies are examined.
- Descriptions of boreholes drilled for the Einstein Telescope site investigation.
- Interlinked uncertainties make a complex dynamic in the uncertainty chain.
- Ambiguity in fracture and bedding dips complicates borehole image interpretation.

Abstract

Geological models are important for subsurface engineering and it is crucial to identify their uncertainties. However, uncertainties in their geological input can be elusive and easily overlooked. Through a data review of Paleozoic geology of the Euregion-Meuse-Rhine, uncertainties in geomodelling inputs are identified and their causes are categorised into four groups: (1) stratigraphic interpretation, (2) fault interpretation, (3) transferring data, and (4) uncertainty in legacy materials. Examining these uncertainties reveals numerous sources for them that are intertwined. The number of connected sources of uncertainty demonstrate that the uncertainty chain in geomodelling is complex, calling for further investigation into the magnitude of the identified uncertainties.

The Paleozoic geology in the study region has structural complexity in which geomodelling is hampered by limited outcrops and scattered input data. We compile input and examine data inconsistencies by collecting legacy literature and maps, conducting fieldwork, and compiling a dataset of 738 boreholes. Stratigraphic profiles of new boreholes (Cottessen-01, Banholt-01, and Terziet-02) are also included and two boreholes (Kastanjelaan-02 and RWTH-01) are re-evaluated with additional palynological constraints. Differences are found between various stratigraphic profiles for the latter two boreholes among different sources and updated stratigraphic profiles are presented for them. Comparing a newly drilled borehole with an existing geological cross-section reveals a >1 km depth mismatch between stratigraphic stages. Comparing stratigraphy of the borehole dataset with different geological maps reveals various degrees of agreement. The identified inconsistencies demonstrate the necessity of validating input data before embarking on any geomodelling exercise.

Introduction

Uncertainty is an inherent aspect of geology which has always been an essential component of subsurface research and geomodelling. Uncertainty that cascades into geological models is one of the most important aspects of the entire geomodelling process and thus, tracking them is pivotal. However, uncertainties in their inputs are elusive and easily overlooked. Therefore, our research question is: What is the origin of *uncertainties in geomodelling inputs?* This article aims to identify the causes of uncertainties after reviewing subsurface data. These uncertainties are important for making geomodels for various subsurface purposes. For example, in the Euregion Meuse-Rhine (Figure 1), geomodels are important for extracting renewable geothermal energy (Mijnlieff, 2020). They are also necessary for establishing energy storage systems (Kramer et al., 2020) and to better understand subsidence and rising groundwater in the former coal mining region (Cuenca et al., 2013; Vis et al., 2020). Furthermore, a geological model is relevant for an ongoing engineering project regarding the construction of a gravitational wave observatory, Einstein Telescope (Burchartz et al., 2025).

The above-mentioned applications illustrate a general need for geologic models. To build these models, choosing the appropriate heterogeneity scale and assessing uncertainty are

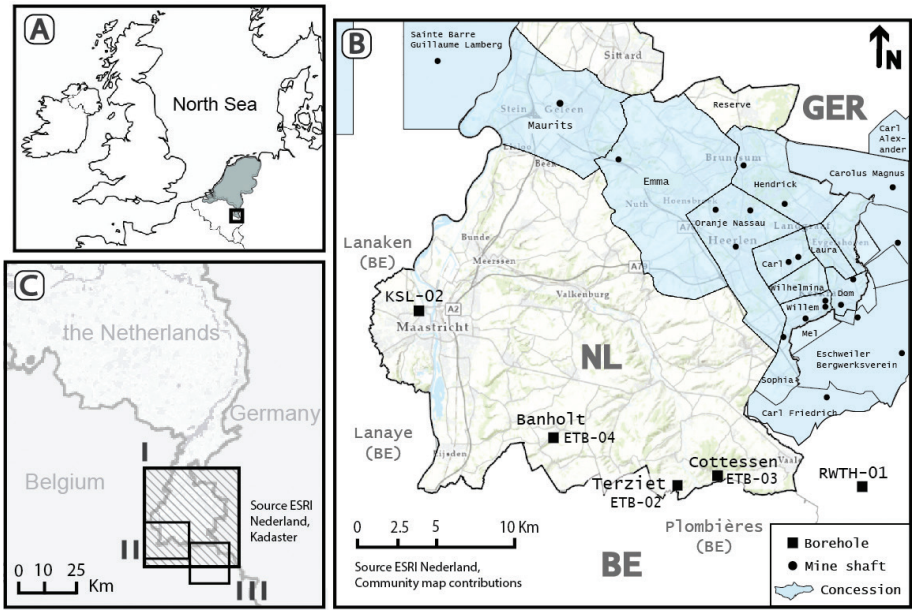

Figure 1. (A) Sketch map of northwestern Europe indicating the study region. (B) Data inventory region with mining concessions and their known entry shafts inferred from RGD (1995). Mel is Melanie, and Dom is Domaniale. Three boreholes drilled for the Einstein Telescope site investigation in the Netherlands are indicated with the code ETB. (C) Map indicating locations of examined geologic maps with black squares; I (RGD, 1995), II (Barchy & Marion, 2007), III (Laloux et al., 2000).

Table 1. Consulted geodatabases and their hyperlinks, last accessed on 01-04-2025.

Geodatabase	Web address
NLOG	https://www.nlog.nl/datacenter/brh-overview
Dinoloket	https://www.dinoloket.nl/en/subsurface-data
DOV	https://www.dov.vlaanderen.be
GSB	https://collections.naturalsciences.be/ssh-geology-archives-plone6/boreholes/descriptions
GD-NRW	https://www.bohrungen.nrw.de
Carte Wallonie	https://geologie.wallonie.be/

crucial (Pyrcz & Deutsch, 2014; Reid & Cowan, 2023; Schweizer et al., 2017). Geomodels are interdisciplinary and regularly intended to perform fluid flow simulations or predict subsurface integrity. When making them, non-communicated uncertainties can add up and permeate into the final model. Most published workflows emphasise uncertainties in the geostatistical process, while uncertainties in geomodelling inputs receive less attention. These inputs can include stratigraphic borehole profiles, geoloigcal maps, and cross-sections (Burs et al., 2016; Burt et al., 2021). Other inputs include well-log data, core data, outcrops, and geophysical survey data. Seismic data acquired, thus far, in the study region is hampered by noise obstructing their interpretation. Therefore, we excluded seismic data and other geophysical survey data from this review. Thus, this review assesses the reliability of non-geophysical survey data necessary to map and understand the cascading chain of uncertainty.

An important source of geomodelling input data comes from records of national geological surveys. In the Netherlands, two different geodatabase viewers provide stratigraphic information. The study region, however, crosses three national borders (Figure 1), for which no unified database exists. Hence, we collected and integrated data from different Dutch, German and Belgian geodatabases (Table 1). These databases are a collective achievement, although the information provided is not guaranteed to match its data source. We compare stratigraphic profiles from these viewers with the original borehole descriptions and later amendments. This comparison serves as an indication of uncertainty in such geodatabase viewers.

To test the validity of geological maps, we examine three maps (Figure 1C; Barchy & Marion, 2007; Laloux et al., 2000; RGD, 1995), focusing mainly on the one map from the Netherlands that covers the complete study region (Figure 2). This is the most recent geologic map showing the top-Paleozoic surface (RGD, 1995). The map succeeded two older maps (Bless et al., 1976; Kimpe et al., 1978) and was published without an explanatory note. The lack of a report obstructs a swift understanding of this map and its underlying assumptions and data. Therefore, five selected structures depicted on the map were traced down in legacy literature to evaluate their uncertainty. Moreover, we compare the map with borehole and outcrop data to identify stratigraphic mismatches.

The majority of legacy materials in the region originates from coal mining activities. During mining operations, hundreds of boreholes were described and a vast amount of knowledge was accumulated. Mines were mapped and cross-sections of the Limburg, Liège, and Aachen coalfields were drawn (Chaudoir et al., 1953; Humblet, 1941; Sax, 1946; Wrede & Zeller, 1988). Although they provide a vast amount of data, unknown uncertainties in such legacy materials can be problematic for the ultimate geomodelling exercise. Therefore, we aim to identify sources of uncertainty in these legacy materials.

Uncertainty can also relate to interpreting stratigraphy and faults in newly acquired data. In the study region, new borehole data are being acquired for a site investigation to possibly construct a gravitational wave detector called Einstein Telescope. This detector is designed to be installed in the subsurface with

https://doi.org/10.70712/NJG.v105.12991

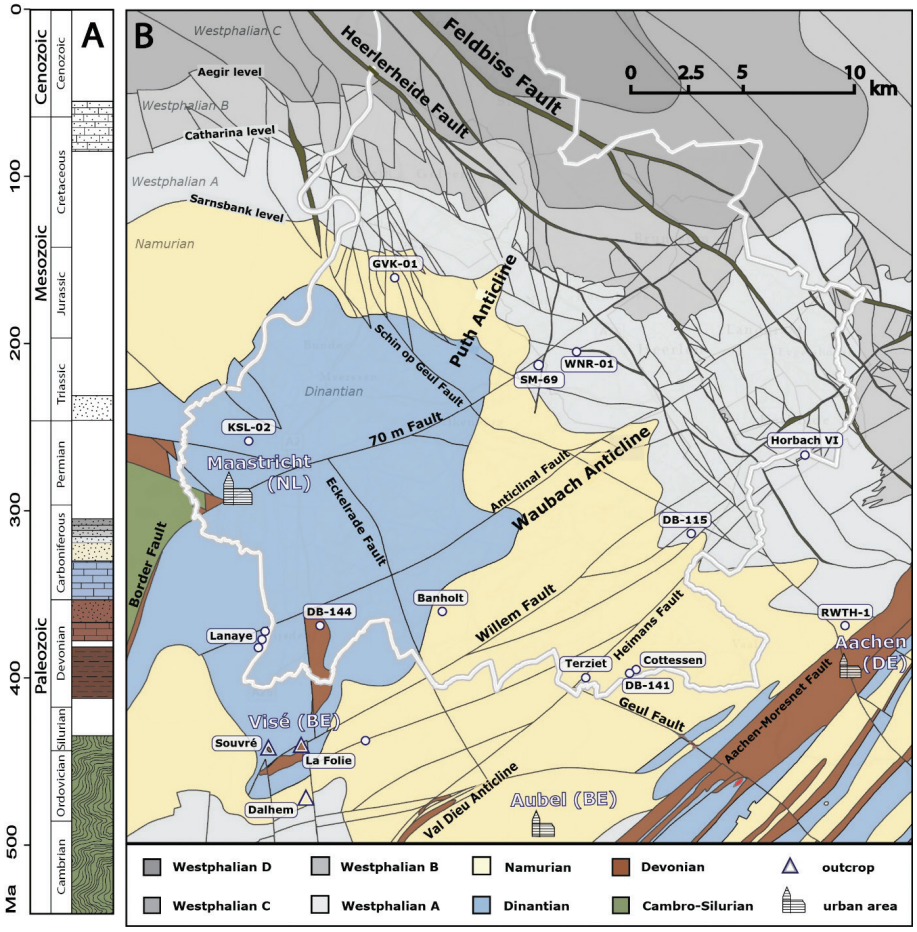

Figure 2. (A) Chronostratigraphic column with an approximate indication of the main depositional phases. (B) Top-Paleozoic map, where Mesozoic and Cenozoic strata are stripped away. Redrawn after RGD (1995). Boreholes discussed in Section 4 are indicated with white circles and outcrops with triangles.

either a triangular or a L-shape with 10–15 km long arms (Branchesi et al., 2023). For derisking and planning, a geological model with assessed uncertainties is called for (Amann et al., 2020). Geological models in structurally complex domains, such as these, can be made with various approaches (Brisson et al., 2023; Wood & Kessler, 2021). All approaches benefit from an understanding of the geological architecture and uncertainty. We examine uncertainties related to interpreting faults and stratigraphy using the first three boreholes drilled for this site investigation. These inherent uncertainties should serve as an opportunity for deepening our understanding of geological limitations. This will hopefully allow for building more reliable geomodels.

Geological setting

Upper Paleozoic rocks in study region cover a Lower Paleozoic basement (Figure 2A). These Paleozoic strata were deformed under northwest-southeast compression by the Carboniferous Variscan orogeny (Wrede & Zeller, 1988). Variscan anticlines and thrust faults formed, which were tectonically overprinted by Mesozoic and Cenozoic normal faulting (Geluk et al., 1995). As a result, the region is characterised by structural heterogeneities whereby thrust faults are offset by normal faults (Hance et al., 1999; Oncken et al., 1999; Sax, 1946). The largest normal fault is the *Feldbiss Fault*, and a substantial thrust is the *Aachen Fault* (Figure 2; RGD, 1995). Structures in the region that are specifically discussed in this article are the *Geul Fault*, *Border Fault*, *Waubach Anticline*, *Visé-Puth Anticline*, and *Val Dieu Anticline* (Figure 2).

Upper Paleozoic strata are covered by Upper Cretaceous deposits separated by a hiatus that covers >200 myrs. During this period, erosion shaped an undulatory peneplain from hard Paleozoic bedrock that shaped the unconformity at the top-Paleozoic surface (Langenaeker, 2000). Quaternary uplift resulted in a modern-day river-incised landscape with Paleozoic rocks exposed in the valleys (Sougnez & Vanacker, 2011). The Paleozoic strata are of Late Devonian and Carboniferous age. Upper Devonian strata that are encountered near Visé (Figure 1) consist of Frasnian carbonates (Kimpe et al., 1978; Pirlet, 1967). Frasnian strata characteristically bear stromatoporoid fossils (Coen-Aubert & Boulvain, 2006). Upper Devonian deposits comprise micaceous fine-grained sand and siltstones of Famennian age (Bultynck & Dejonghe, 2002; Thorez, 1977). Typical Famennian plant fossils were described from an exposure in the Belgian village Moresnet (Hellemond et al., 2019; Stockmans, 1948). The lower Carboniferous strata (Tournaisian and Visean: Dinantian) consist of dolomites and limestones, commonly with crinoid fossils (Kasig, 1980). In the Belgian and German parts of the study region, these limestones have a karstified top with cavities filled with upper Carboniferous deposits (Kasig, 1980; Poty, 1991). Upper Carboniferous strata (Namurian and Westphalian) comprise siliciclastics that host coal seams and frequent plant fossils (Bless et al., 1980a). Upper Carboniferous strata are known from

https://doi.org/10.70712/NJG.v105.12991

the coalfields and outcrops (Figure 1b; Jongmans et al., 1925; Walter, 2010). These strata consist of a mudstone succession of Namurian age with an organic-rich base (Nyhuis et al., 2016; Wei et al., 2023) and fluvial-deltaic deposits of Westphalian age (TNO-GDN 2025d).

Stratigraphic nomenclature of the Paleozoic is subject to progressive insight and recent changes (Mottequin et al., 2024; Vis et al., 2025). A harmonised stratigraphic nomenclature is not available for this region straddling national boundaries. For Carboniferous units, this study uses the Dutch lithostratigraphic nomenclature (TNO-GDN, 2025a, b, c, d) following Van Adrichem Boogaert and Kouwe (1994), and recently proposed updates (Vis et al., 2025). The nomenclature of Mottequin et al. (2024) is used for Devonian units, resulting in the use of *Condroz Formation* for Famennian micaceous sandstones. Proposed units are written here uncapitalised and ratified formations are capitalised. For fault rock terminology, we adhere to the scheme of Woodcock and Mort (2008). We also adhere to the formally used global timescale (Cohen et al., 2023), except for the Carboniferous. The Carboniferous has been defined differently according to various schemes (Davydov et al., 2012), and a harmonised classification is problematic (Aretz et al., 2020). To avoid stratigraphic confusion with regional literature, we chose to deviate from the formal timescale for the Carboniferous and adhered to the European nomenclature, based on the Heerlen regional scheme (Jongmans, 1928; Jongmans & Gothan, 1937). In contrast to the formal Mississippian and Pennsylvanian subsystems (Gradstein & Ogg, 2020), this regional nomenclature divides the Carboniferous into Dinantian and Silesian. These subsystems are, in turn, divided into series; the Dinantian is split into Tournaisian and Visean, and the Silesian into Namurian, Westphalian, and Stephanian. This regional division is still deemed valid for regional units (Aretz et al., 2020).

Materials and methods

Three work steps were followed: (1) collect geomodelling input data and materials, (2) identify uncertainties, and (3) categorise types of uncertainties. We define uncertainty as: 'the recognition that information may deviate from reality' (Merriam-Webster, n.d.). To identify uncertainty we test the consistency of how data are presented and processed. For the latter new data are analysed.

Data compilation

Literature, borehole and outcrop data, and maps were collected to create the necessary data overview. Borehole data were gathered from various publicly accessible data sources: (1) TNO-Geological Survey of the Netherlands geodatabases (NLOG and Dinoloket), (2) database ondergrond Vlaanderen (DOV), (3) archives from the Geological Survey of Belgium (GSB), (4) survey of Nordrhein-Westfalen (Geobasis NRW), and (5) database viewer of Wallonie (Table 1). For the remaining borehole data, which were absent in geodatabases, we inferred coordinates from vectorised maps using ArcGIS® (ESRI, 2016). We converted all coordinates to Amersfoort / RD new projection (EPSG code 28992).

Legacy literature consists of annual reports and notices from geological surveys. Reports include dissertations and legacy borehole reports, accessed from the archives of TNO-Geological Survey of the Netherlands and the Geological Survey of NRW. In addition, cross-sections from the Limburg coal mines were evaluated.

New data

Cores and boreholes

Borehole data, acquired for the Einstein Telescope feasibility study, were described to characterise cores and cuttings. We focus on stratigraphic boundaries and fault zones. A total of 10% hydrochloric acid (10% concentration) was used to identify calcite, and grain sizes were observed using a hand lens (10x). Grain sizes are grouped according to the Wentworth classification (Wentworth, 1922). Dip angles of bedding planes were determined in core using a protractor, assuming that cores were cut at right angles to the bedding.

Borehole image logs were analysed to recognise dip and fracture patterns. Well-log data were recorded by Terratec Geophysical Services GmbH and include spectral gamma-ray logs, televiewer and acoustic images. These oriented borehole images were studied to identify faults by picking bedding surfaces using software (WellCAD, 2022). Bedding planes were recognised as dark blue parallel layering in the acoustic amplitude logs and shaded parallel layering in the optical logs. After picking, our interpretation was compared with the core to validate the image log interpretation and identify potential pitfalls when using borehole image logs.

Palynological analyses

Palynological analyses on samples taken from cuttings, cores, and outcrops were conducted by A.J.P. Houben. A total of 52 rock samples were processed at CGG Laboratories, Conwy, United Kingdom. Microscope slides were studied with a transmissive light Leica DM-LB2 microscope at the Geological Survey of the Netherlands. Palynological observations and ensuing interpretations are displayed in the range charts provided in Supplement 3. For each palynormph, a confidence assessment for each interpreted interval was assigned with the categories: low, medium, and high confidence.

Evaluating legacy materials

Examined legacy materials are articles, documents, photos, maps, and cross-sections mostly made in the 20th century (Figure 3). These legacy data and concepts are accumulated by decades of work by mining geologists and efforts of geological surveys (Geologisch Bureau Heerlen, GSB, and Geologischer Dienst NRW). Fossils were described (Dorsman, 1945; Jongmans & Robert, 1917) , lithostratigraphic correlations were made (Haites, 1948), and tectonostratigraphic overviews were published (Bless et al., 1980a). In addition, anticlines, synclines, and faults were interpreted (Bless et al., 1976; Dikkers, 1945; Sax, 1946). A subset of two interpreted anticlines (*Waubach Anticline and Visé-Puth Anticline*) and two faults (*Border Fault and Geul Fault*) depicted on geological maps are evaluated in this study (Figure 2).

To test the validity of materials, we compared them with original reports or data. To test borehole descriptions, cores of Kastanjelaan-2 were logged and compared with the original description (Bless et al., 1981a). To test geodatabase viewers,

https://doi.org/10.70712/NJG.v105.12991

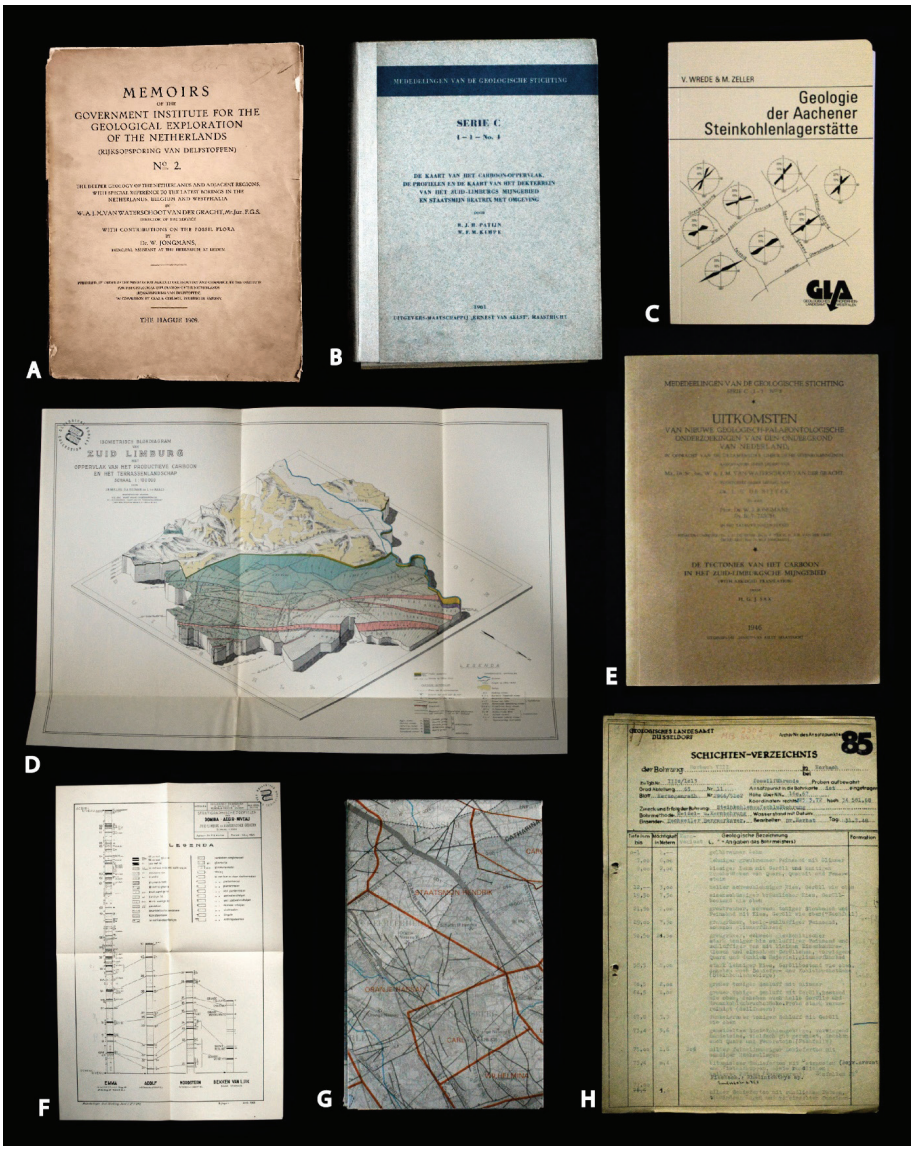

Figure 3. Examples of legacy materials. (A) Cover of early literature on regional Paleozoic geology (Van Waterschoot van der Gracht, 1909). (B) Document appending a top-Paleozoic map (Patijn & Kimpe, 1961). (C) Literature on the Aachen coalfield (Wrede & Zeller, 1988). (D) Isometric block diagram of the South Limburg coalfield (Sax, 1946). (E) Literature on the South Limburg coalfield (Sax, 1946). (F) Stratigraphic profiles of coal mines and their correlations (Haites, 1948). (G) Folded top-Paleozoic map (RGD, 1995). (H) Example of a borehole description of Horbach VI (Herbs, 1948).

their stratigraphic information was compared with original reports and later amendments. Moreover, borehole data were compared with the most recent top-Paleozoic map (RGD, 1995). Furthermore, borehole data were compared with cross-sections published with geological maps (Barchy & Marion, 2007; RGD, 1995) and inventoried outcrops were used for mapping. Based on these outcrop data, borehole data, and legacy literature, four structural elements depicted on this geological map were evaluated. These elements are: *Border fault*, *Geul Fault*, *Waubach anticline*, *Visé-Puth anticline*, and the *Val Dieu Anticline*.

Data overview

The assessment of legacy materials and processed data is not intended as a critique, but as a necessary step to understand uncertainty in modern geomodelling practices using such data. We recognise that various factors, such as time and data limitations, may have caused uncertainty in the past and that knowledge progresses over time. Also, the research goals of past studies did not necessarily require serving as geomodelling input.

Mining materials

In the South Limburg coalfield, over 7000 drillings were taken upwards in the roofs of mining galleries to determine the height between galleries and the top-Paleozoic surface, or to explore coal seams (Dikkers, 1945). These drillings reached lengths over 50 m, and most were cored, although none of them remained physically archived. Mining galleries, shafts, and drillings were logged, of which the shafts were described in most detail (Dikkers, 1945; Figure 4A). Differences have been described between logged shafts and nearby borehole logs in the Maurits concession (Dikkers, 1945). These differences could suggest uncertainty in mining logs. Yet, a description of numerous upward drillings exists (n = 7228), making them useful for modelling purposes, such as modelling the depth of the top-Paleozoic surface.

Based on a mapping campaign of the mines, an isometric block diagram and a top-Paleozoic map were created (Sax, 1946; Figure 3D). Faults were categorised into three groups, namely SE-NW oriented normal faults, SW-NE oriented thrust faults, and an enigmatic group of NS-oriented faults (Sax, 1946). Among these faults is the *Willem Thrust* which is regarded

https://doi.org/10.70712/NJG.v105.12991

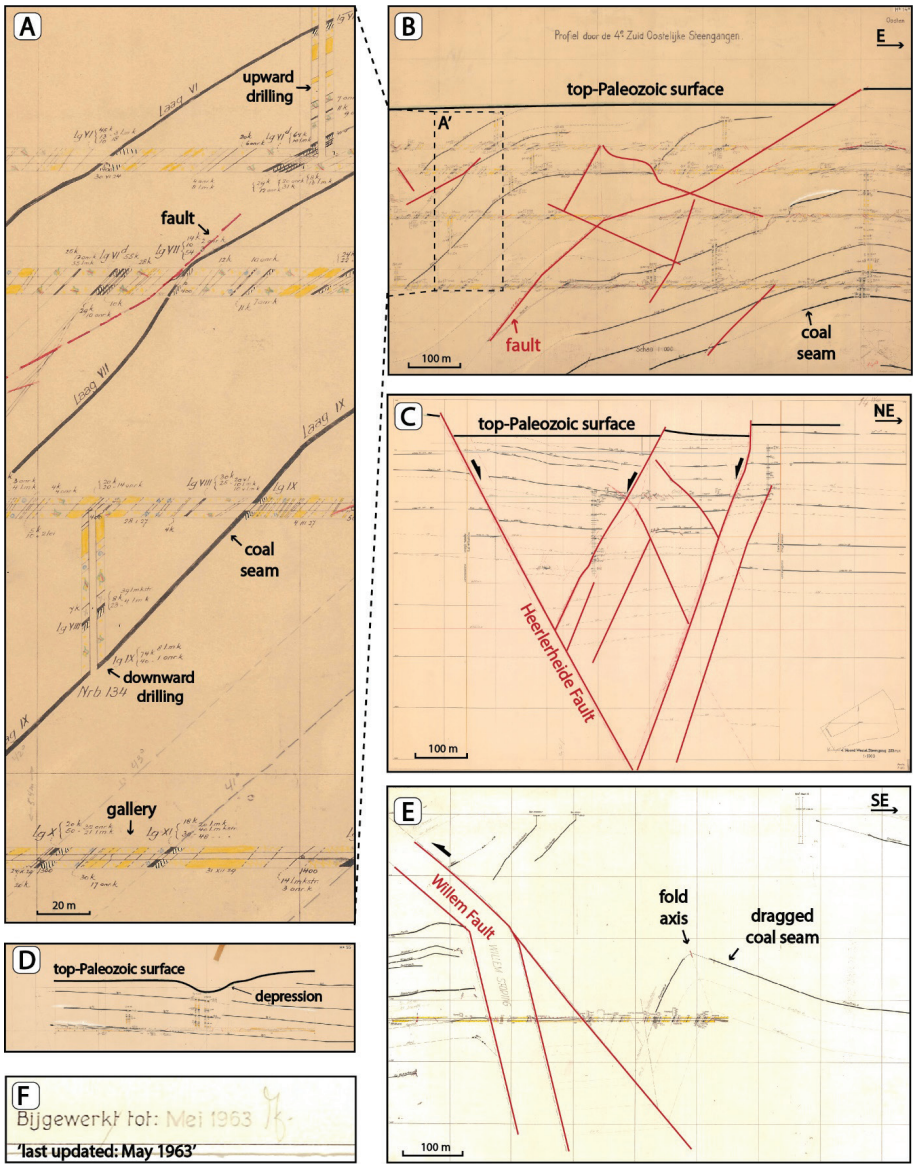

Figure 4. Cross-section scans from the South Limburg coalfield providing information on geological structures with varying reliability. Faults are drawn over in red. (A) Detail of cross-section B, showing logged shafts, drillings, and galleries. (B) Cross-section from the Hendrik Mine showing fault geometries lacking offset. (C) Cross-section from the Wilhelmina Mine. (D) Cut from a cross-section of the Hedrick Mine showing a depression in the top-Paleozoic surface. (E) Cross-section of the Willem Mine showing the *Willem Fault* with dragged coal seams in the hanging wall providing a sense of structural style. (F) Indication of the date of the last update in a period of gradual paradigm shift (Nitecki et al., 1978). Concession localities are indicated in Figure 1.

as one of the most substantial thrusts (Sax, 1946). This fault is described with a 300 m throw (Sax, 1946), as depicted in cross-sections (Figure 4E). The dragged coal seams on this cross-section have the shape of a hanging wall anticline and thus, provide a sense of structural style. These cross-sections were updated until the 1960s (Figure 4F), when the paradigm gradually shifted to accepting plate tectonic theory (Nitecki et al., 1978). Before this shift, the processes of faulting were generally interpreted differently, causing uncertainty in legacy cross-sections.

Cross-sections resulting from the rigorous work of coal mining geologists can be useful to locate faults in the subsurface. For example, a cross-section from the Wilhemina Mine shows a normal fault with conjugate sets (Figure 4C). Cross-sections also provide other helpful information such as channel-shaped depressions cutting the top-Paleozoic surface (Figure 4D). However, some cross-sections show geometries that are geometrically unlikely (Figure 4B) such as faults lacking any offset. Unlikely cross-section may result from a different understanding of tectonic processes before the 1960s (Nitecki et al., 1978). Hence, cross-sections can provide relevant information about faults, although some care is needed.

Outcrops

Over 58 outcrops are still exposed along river valleys, while 154 outcrops (Figure 5) can be inferred from geological maps (Barchy & Marion, 2000, 2007; Laloux et al., 2000; RGD, 1995) and literature (Jongmans et al., 1925; Walter, 2010). Outcrops are clustered along a northwest-southeast trajectory in the Geul river valley and the region near Visé, Dalhem, and Val Dieu (Belgium; Figure 5).

https://doi.org/10.70712/NJG.v105.12991

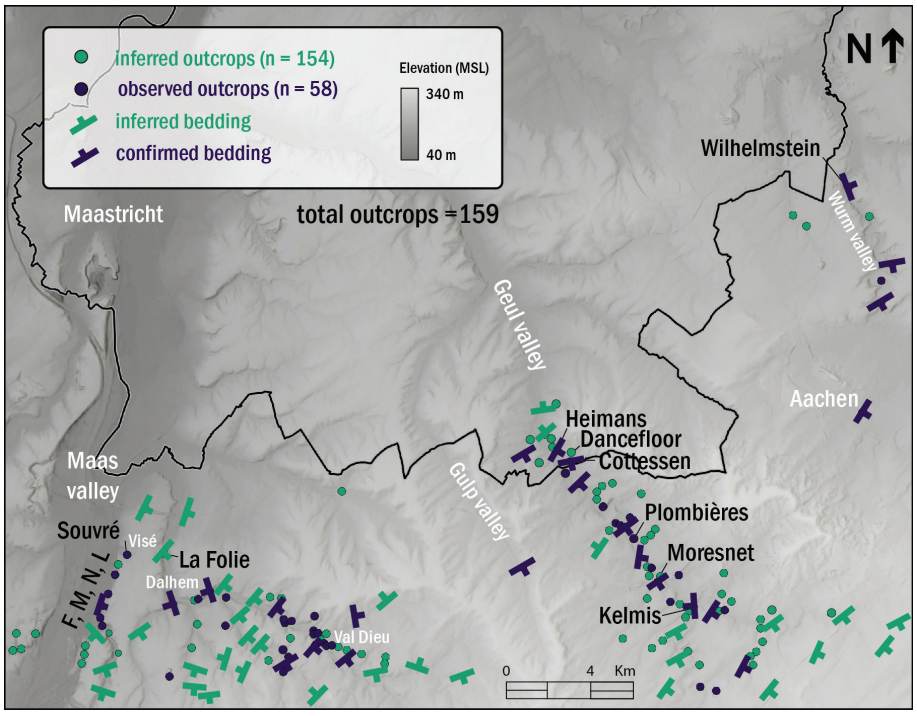

Figure 5. Digital elevation model (MAPS for Europe, n.d.) with Paleozoic outcrop locations and their bedding attitude indicated. Green symbols indicate outcrops inferred from geologic maps (Barchy & Marion, 2000, 2007; Laloux et al., 2000; RGD, 1995) and literature (Jongmans et al., 1925; Walter, 2010). Purple symbols were confirmed in recent fieldwork. Former carbonate quarries in the Maas valley are referred to as F,M,N,L (Pirlet, 1967). For measurements, see Supplement S1.1 and for the elevation model, Supplement S4.3.

Geul river-valley

Paleozoic strata are exposed along the Geul river-valley (Figure 5). Examples are the former Heimans, Cottessen, and Kamp quarries in the Netherlands, where sandstones of Namurian age were mined (Jongmans et al., 1925). The Kamp quarry is currently overgrown, yet archived photos from the Geological Survey of the Netherlands show deformed strata (Figure 6B) described as shales and sandstones (Thiadens, 1948). Shales also occur in the Heimans quarry as part of an open fold with a 57° striking axis. This fold is still exposed, although archival photos show twice as many outcropping strata than currently accessible (Figure 6A). Furthermore, shales and quartz conglomerates are exposed in the Cottessen quarry, as well as southeast-northwest oriented slickensides (135°/31°). We measured similarly oriented slickensides (145°/12° and 122°/2°) in two outcrops south of the church in Plombières (Belgium), with steps indicating sinistral strike-slip movement. Namurian strata are also exposed directly north of Sippeneaken and in a former quarry at Terbruggen (Delmer & Graulich, 1959). The outcrop at Sippeneaken is still accessible and exposes steeply dipping siltstones, while the former quarry at Terbruggen is closed off by a fence.

At Plombières (Belgium), Dinantian and Namurian strata are indicated on the top-Paleozoic map (RGD, 1995). The Dinantian strata in Plombières hosted a Pb-Zn ore (Bevandić et al., 2020; Dejonghe, 1998), depicted with an elongated NW-SE oriented shape on the RGD (1995) map. Archival photos show an outcrop with tightly folded Dinantian strata (Figure 6D). This outcrop is now largely overgrown, although bedding (054°/38 SE) and a fold axis (060°/08° ENE-WSW) are still measurable. Near Plombières, three more outcrops are indicated along a tributary of the Geul river, which are currently all overgrown and inaccessible. Similarly, the classic outcrop at Moresnet (Figure 5), Suermondt quarry, is no longer accessible due to waste dumping. Nevertheless, literature (Hellemond et al., 2019; Stockmans, 1948) confirms the former existence of this exposure. These inaccessibilities of former outcrops introduce an uncertainty caused by limited data availability.

Near Moresnet, Dinantian carbonates described by Conil (1964) are still exposed and Dinantian strata also crop out along the N3 road in Kelmis (Figure 6). In the latter outcrop, a sub-vertical fault plane with north-south oriented slickensides (008°/30°) is exposed and strata are steeply inclined (60–81°) with a deviating westward dip (Figure 5). A similarly deviating strike of 339° was also measured at the Wilhelmstein outcrop along the Wurm valley (Figure 5). These deviating bedding attitudes indicate structural complexities.

Visé, Dalhem, and Val Dieu

Carbonates of Frasnian and Dinantian age are exposed in quarries along the eastern bank of the Maas River parallel to the E25 motorway near Visé (Horion & Gosselet, 1892; Poty & Delculée, 2011). Frasnian carbonates are described in the former La Folie and Souvré quarries (Figure 2; Kimpe et al., 1978; Plisnier, 1931). Both quarries are now private property, which hampers a detailed inspection. Nevertheless, some overgrown Frasnian is exposed along a steep slope at Souvré, but the bedding is unrecognisable. The Frasnian at Souvré is described as 'puzzle breccia' with massive stromatoporoids (Kimpe et al., 1978) and at the La Folie quarry as Frasnian dolomites and shales (Pirlet, 1967). Despite the inaccessibility of these outcrops, literature confirms their existence and provides stratigraphic constraints in agreement with geological maps (Figure 2; Barchy & Marion, 2007; RGD, 1995).

https://doi.org/10.70712/NJG.v105.12991

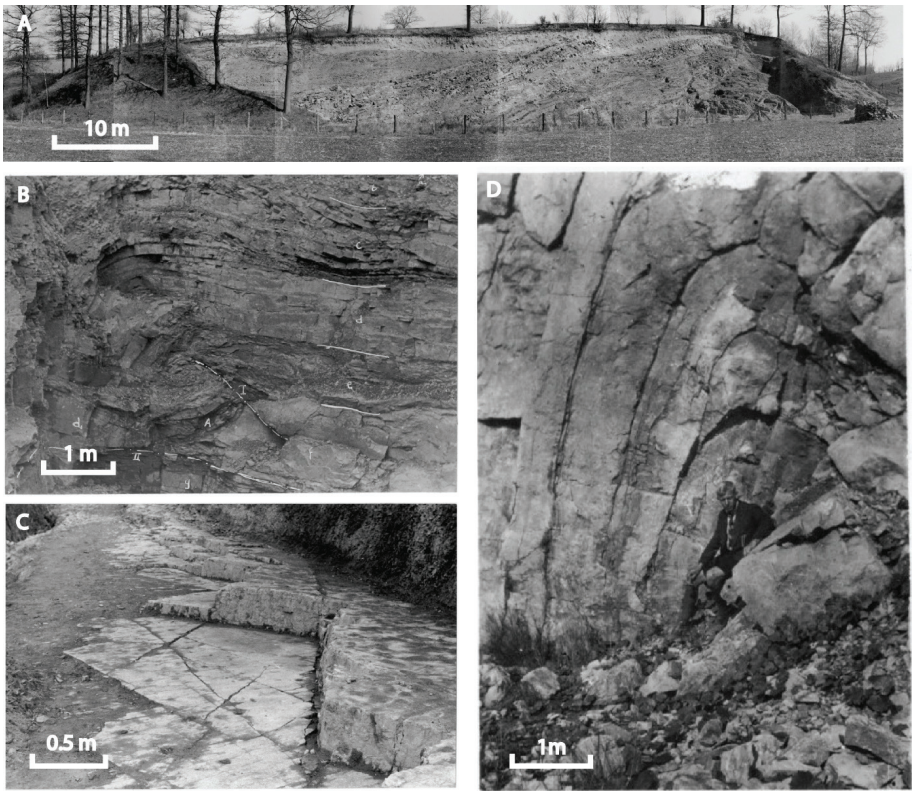

Figure 6. Photos of outcrops that are now inaccessible or partly overgrown. (A) Photo assemblage from the Heimans quarry in 1936. (B) Photo of the Kamp quarry in 1948. (C) Namurian strata at the 'Dancefloor' outcrop from 1945. (D) Photo from 1937 showing folded Dinantian strata at a former mine in Plombières; note the sitting person for scale. Photos are accessed from the TNO-photo archive; locations are indicated in Figure 5.

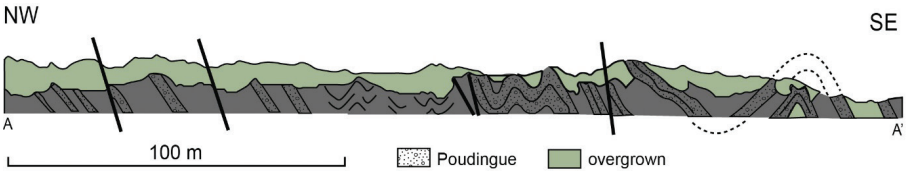

Figure 7. Sketch of the Dalhem-Val Dieu road section after Raucq (1942). Sketch shows >100 meters more Namurian strata outcropping than is currently exposed, demonstrating how an assessment of legacy materials can be obstructed. See supplement S5 for location.

Near Dalhem (Belgium), Namurian and Lower Westphalian strata are exposed (Lambrecht, 1966). A sample for palynology from an outcrop at the southern exit of tunnel in Dalhem (Figure 5), yielded rich yet poorly preserved miospores. Spore colouration is dark and the sample is dominated by long-ranging Late Carboniferous and younger spores (Supplement S3.7), which indicate a Westphalian age with an imprecise range (SS-Zone or RA-Zone of Clayton et al., 1977). A Westphalian age mismatches the most recent top-Paleozoic map at this location (Figure 2), however, unambiguous marker taxa for this Westphalian zone were unidentified. Thus, this age interpretation comes with uncertainty.

Outcrops along the road from Val Dieu to Dalhem expose Namurian strata concordantly overlying Famennian strata (Ancion et al., 1943). Famennian strata comprise fine micaceous sandstones with regular planar lamination and plant fossils. Two sections are cut along the road, of which the one closest to Val Dieu abbey exposes a thrust fault (334°, 22° ENE) with metre-scale offset. Another section shows Famennian strata (043°, 40° NW) as part of a fold and an outcrop exposes contorted and tightly folded Namurian mudstones. In legacy literature, the road section is sketched, showing >100 meters more outcrop than currently exposed (Figure 7: Raucq, 1942).

Borehole data

Boreholes in Belgium, Germany, and the Netherlands are compiled into one dataset. Shapefiles of this dataset is provided in the supplementary materials. Rendering all borehole data onto one map revealed a clustered and uneven distribution over the study region (Figure 8). Most boreholes are located in the former South Limburg and Aachen coalfields or where Paleozoic strata are subcropping at shallow depths. Exploration boreholes, Exploration boreholes at Pb-Zn ores near Plombières and Moresnet, also exist, however, these are left out related to data accessibility.

New boreholes

Cottessen (ETB-03)

In 2022, the 250.1 m deep, fully cored, Cottessen borehole was drilled near the Dutch-Belgian border for the Einstein Telescope

https://doi.org/10.70712/NJG.v105.12991

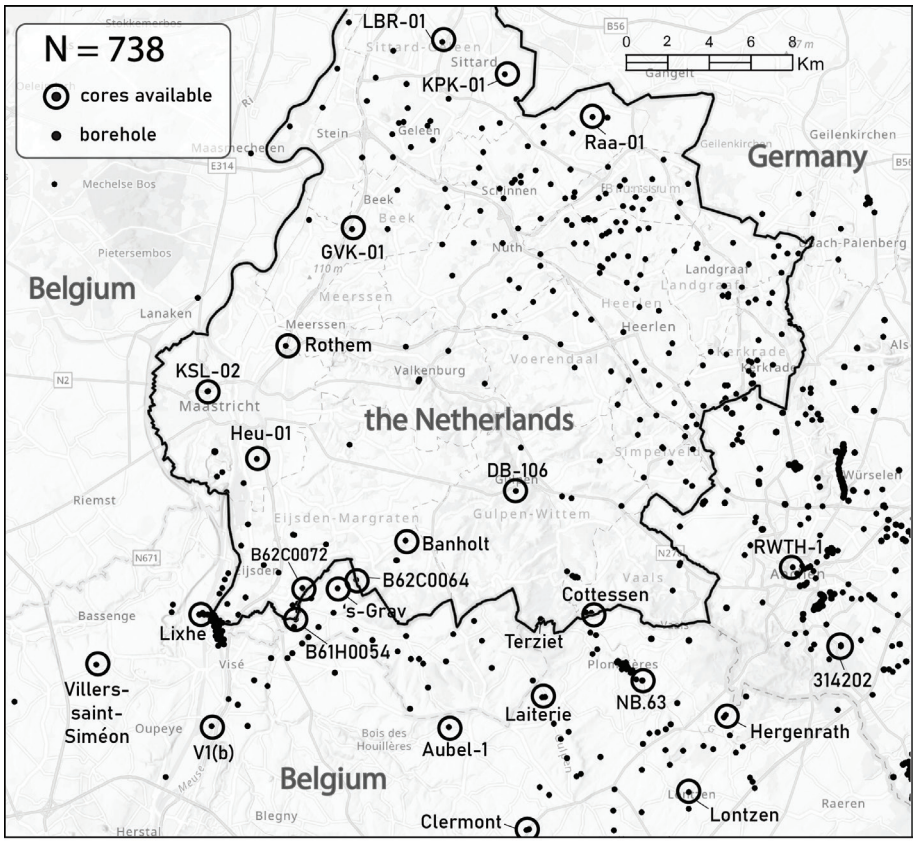

Figure 8. Map showing 738 boreholes in South Limburg and its surroundings that reached Paleozoic rocks. Circled boreholes have cored samples available, of which DB-106, Laiterie (123W-724), and Villers-Saint-Siméon (121W-220) only have hand specimens. Banholt, Cottessen, Terziet, and Aubel-1 were newly drilled for the Einstein Telescope site investigation. 's-Grav = 's Gravenvoeren. Note the uneven data distribution with most boreholes located in the coalfields or where Paleozoic strata are shallowly subcropping.

feasibility study, known as E-Test (Interreg EMR, n.d.) (Figure 9). A gamma-ray log was acquired over the full borehole trajectory and optical and sonic borehole image logs were acquired from 35 to 250.1 m depth. The borehole encountered a 53.6 m thick succession of dark shales with faint lamination and thinly alternating fine sands and mudstones (Supplement S2.2). Based on palynology (Supplement S3.2), the interval above the lithostratigrpahic contact at 53.6 m (Fig. 9) suggests an early Namurian age. Therefore, we interpret this succession as pertaining to the Epen Formation. Underlying this succession are micaceous fine to very fine sandstones and thinly alternating fine sand and mudstones with frequent burrows. The micaceous sandstones are either massive, planar laminated, wavy laminated, or cross-laminated. Moreover, soft-sediment deformation such as slumps and loading structures occurs. Based on these lithofacies, this succession from 53.6 to 250.1 m is interpreted as the Condroz Formation. New palynological data indicate that this interval is of middle-late Late Famennian age (Supplement S3.2). Collectively, these bio- and lithostratigraphic interpretation imply an unconformity at 53.6 m separating the middle-late Late Famennian from the Namurian.

Bedding attitudes inferred from borehole image logs (strike = 80°) in the top interval (35–75 m) agree with those in the nearby Cottessen quarry (strike = 74°). This agreement validates the orientation of the borehole images. Yet, the Famennian-Namurian unconformity in the core has an annotated depth of 53.6 m, whereas it is recognised at 52.8 m in borehole images (Figure 9D). This difference corresponds to a 0.8 m core shift between the core and borehole image logs. This core-log shift introduces an imprecision in the depth of bounding surfaces if the shift is not taken into account.

A comparison of our borehole image log interpretation and the actual core revealed that low-angle veins (Figure 10E) were unrecongised in the image logs (Figure 10D). Also, no vertical strata were interpreted from image logs, despite their presence (Figure 10E). Therefore, it is likely that fractures oriented roughly parallel to the bedding were confused with the bedding itself. This similarity between bedding and fractures in image logs causes uncertainty in fracture characterisation. This imprecision can be corrected for by calibrating recognisable structures in the core to the depth indicated by the image logs.

Trends in dip patterns recognised in the core match dip patterns inferred from image logs (Figure 10B). These dragged dip patterns indicated three thrust fault zones at 90.4–108 m, 156–171.9 m, and 203–221.6 m (Figure 10). These zones correspond to broken and heavily fractured strata with abundant veins, fault breccias and clayey gouge (Supplement S2.2). Thus, the comparison between faults interpreted from borehole image logs and the core demonstrated usefulness in identifying fault zones.

Banholt (ETB-04)

In 2017, a 252.8 m deep borehole was drilled near the village of Banholt for the Einstein Telescope feasibility study, known as E-Test (Interreg EMR, n.d.). The 142–230 m interval was cored and a gamma-ray log and acoustic borehole images

https://doi.org/10.70712/NJG.v105.12991

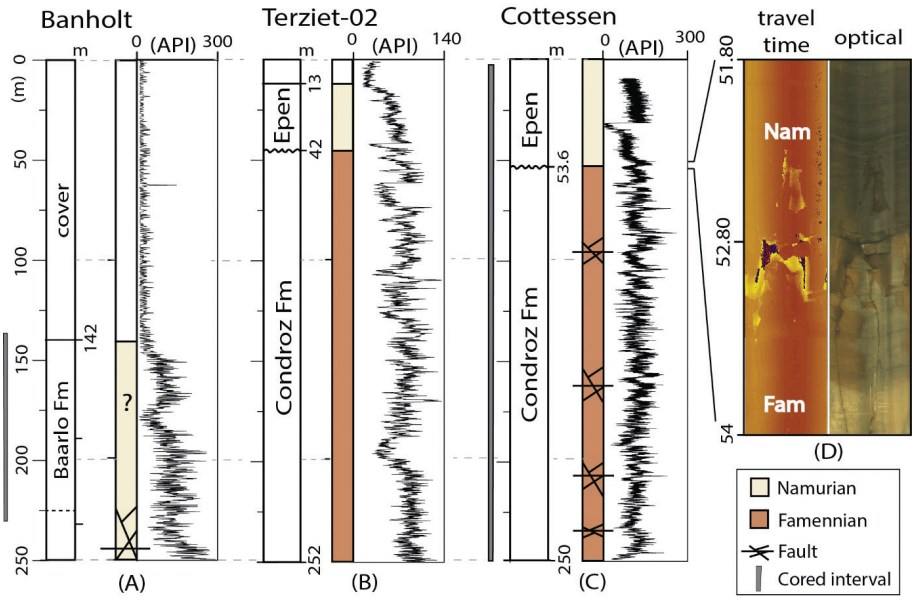

Figure 9. Stratigraphic profiles and gamma-ray logs of three boreholes drilled for the Einstein Telescope feasibility study. (A) Banholt (B62C1327), (B) Terziet-02 (B62D1113), (C) Cottessen (B62D1181), (D) Borehole image logs of Cottessen showing the unconformity between Namurian (Nam) and Famennian (Fam) strata. These profiles are based on litho-stratigraphic descriptions and palynological constraints (Supplementary Materials 2 and 3).

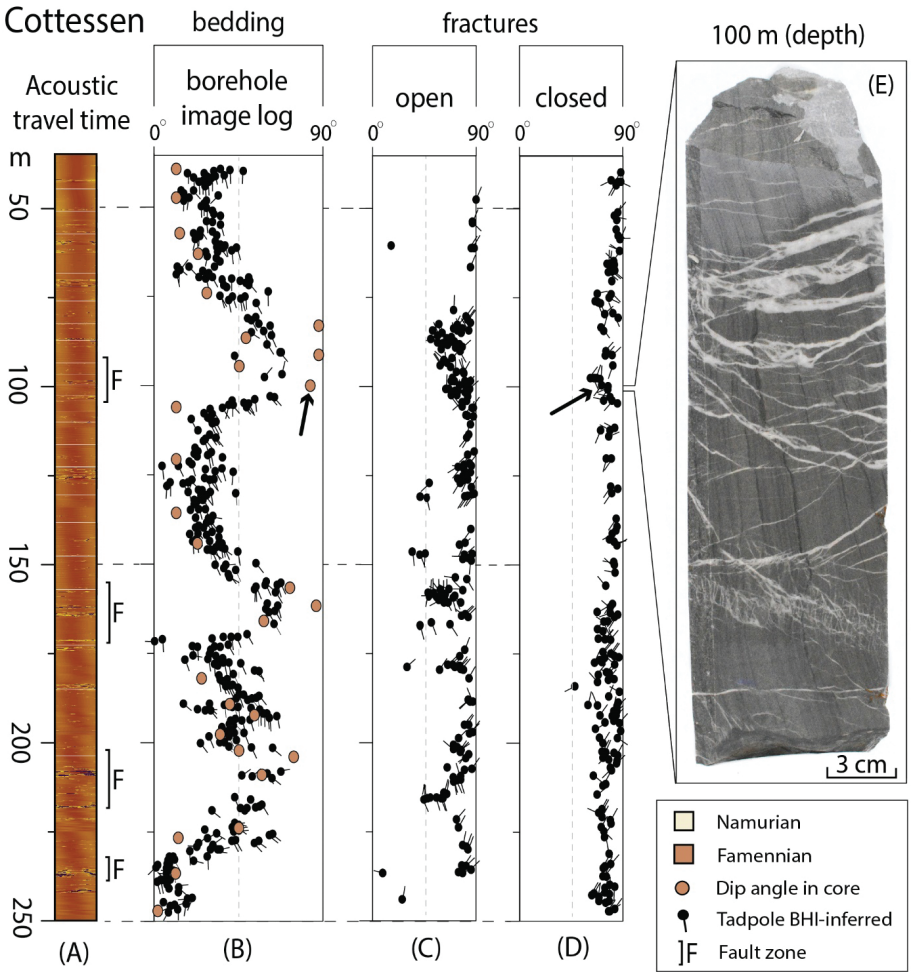

Figure 10. (A) Acoustic travel time image log of the Cottessen borehole (B62D1181). (B) Comparison between bedding inferred from image logs and cores. (C) Tadpoles of open fractures. (D) Tadpoles of closed fractures. (E) Core piece at 100 m depth showing steeply dipping strata and low-angle veins. The arrow indicates a mismatch between the borehole image log interpretation and the core. Note that no vertical bedding and low-angle closed fractures were inferred.

https://doi.org/10.70712/NJG.v105.12991

were acquired. Four core samples were processed for palynology, however, all samples lacked discernible palynomorphs (Supplement S3.3). Strata in the core consistently dip 20–45° with a gradual increase downcore. Strata consist of grey to dark grey mud- and siltstones and coaly intervals of up to 70 cm (Supplement S2.4). These coaly intervals are not only typically found in Westphalian strata but also occur in the Namurian strata of the Dutch Baarlo Formation (NLOG, 2025). The core encountered massive mudstones lacking marine marker beds, thus limiting the lithostratigraphic interpretation. Yet, based on what is predicted on the geologic map (RGD, 1995), we deem a Namurian age interpretation favourable. However, this interpretation is uncertain.

Core in the basal 230–250 m interval was not recovered due to complete core loss of which the cause is unreported. Above this lost interval occurs a 13-meter thick interval of broken claystone, siltstones and fine- to coarse-grained chaotic breccias (Figure 11D). Borehole image logs in this unrecovered interval reveal fractured strata until 243 m depth. Downhole, a 20 cm thick void, oriented bedding parallel, is revealed at 234.8 m. Below this surface neither bedding nor fractures are recognisable and the acoustic signal is chaotic (Supplement S2.3). We interpret the basal 25 m of the Banholt borehole as a fault zone.

Encountering this fault zone raises the need to understand its scale in three dimensions. The fault zone thickness (>25 m) provides a rough estimation, however, this thickness is apparent due to the angle between the fault plane and the vertical borehole. Therefore, the thickness of the encountered fault overestimates the actual thickness. Linking the fault zone thickness to fault dimensions is also not straightforward. Empirical relationships often show substantial scatter (Sperrevik et al., 2002; Torabi & Berg, 2011) and a single fault zone changes thickness along its plane (Caine et al., 1996). Additionally, as drilling stopped in the fault zone, it is unknown whether the fault juxtaposed different stratigraphic units on top of each other, further limiting our understanding. Thus, the scale of the fault encountered in the Banholt borehole is unknown.

Terziet-02 (ETB-02)

Near the Dutch-Belgium border at Terziet two boreholes were drilled 64 m apart from each other. Terziet-02 (B62D1113) was drilled vertically after Terziet-01 (B62D1112) was drilled with an unintended ~6° southward inclination (Supplement S2.1). The Terziet-02 borehole reached a total depth of 252 m and not core but cuttings and a gamma-ray log were acquired (Figure 9b). The borehole encountered dark mud and siltstones from 13 to 42 m, whereas micaceous siltstones were recognised in the strata below 42 m. These micaceous siltstones are characteristic of the Condroz Formation and are thus interpreted as such. Based on palynology (Supplement 3.3), an early-middle Late Famennian age (GF-Zone; Streel et al., 1987) is suggested for the interval of below 42 up to 139 m, and a late Late Femennian age (VCo-Zone; Streel et al., 1987) for deeper strata. The dark mud and siltstones above 42 m are of Namurian age and are typical of the Epen Formation (TNO-GDN, 2025c), and thus interpreted as such. These new litho- and biostratigraphicaphic constraints imply an unconformity at 42 m separating Upper Devonian strata and upper Carboniferous strata (Figure 9).

Inspected cores of legacy boreholes

Kastanjelaan-2 (KSL-02)

In 1981 in the city of Maastricht, the 500 m deep Kastanjelaan-2 (KSL-02) borehole was drilled. Wireline logs, including a neutron and gamma-ray log, were acquired. The interval below 334.7 m depth was cored. This cored interval was initially described by Bless et al. (1981a), which included a biostratigraphic inventory. More recently, the interval consisting of Dinantian carbonates was re-examined, focusing on Dinantian strata (Mozafari et al., 2019).

As Mozafari et al. (2019) excluded Famennian strata at the base, we revisited the cored interval from 377 to 500 m (Supplement S2.5). We analysed five samples for palynology to validate and further refine the interpretations by Bless et al. (1981a).

Famennian strata are characterised by micaceous siliciclastics with various sedimentary structures (Supplement S2.5). In addition, burrowed horizons and conglomerate intercalations are present. An interval of burrowed carbonate-mudstone alternations is present from 465.40 to 459.30 m (Figure 11). The top of this burrowed interval is cut by a normal fault (459.3–452.3 m) containing chaotic breccias (Figure 11D, E) and shear fractures (Figure 11C). The strata above this fault comprise crinoidal-rich carbonates (Figure 11B) and a ~2 m thick interval of dark-coloured carbonate mudstones at 446.30–444 m. Based on the sharp contrast in lithofacies above and below the fault zone, we interpret the centre of the fault (456 m) as the contact between Condroz Formation and the Hastière formation (Figure 12).

Palynological zonations of the Devonian-Carboniferous boundary interval are challenging and its biozonal schemes underwent modifications since the first description of Kastanjelaan-2 (Becker et al., 1974; Denayer et al., 2021; Maziane et al., 1999; Marshall et al., 2018). This prompted a (bio) stratigraphic evaluation (Supplement S3.6). The results of this evaluation imply that the uppermost Famennian, i.e. Strunian, is encountered below 447.55 m depth. In addition, a fault zone at 452.1-458.8 m was recongised to juxtapose crinodional carbonates on to mica-rich siliciclastics (Fig 12A). The above results imply that the Devonian-Carboniferous boundary is located within the crinoidal-rich carbonates provisionally assigned to the Hastière formation (Figure 12A). Thus, we found no evidence to deviate from the originally allocated depth of the Devonian-Carboniferous contact at 445 m (Bless et al., 1981a; Figures 11 and 12). Yet, as palynomorphs could be reworked, we cannot exclude the possibility that the Devonian-Carboniferous boundary is actually located deeper corresponding to the fault zone as a tectonic contact (Figure 11). Thus, the precise depth of the Devonian-Carboniferous boundary comes with some uncertainty.

In the original report, the 382–500 m interval was grouped as Bosscheveld formation (Bless et al., 1981a). To facilitate cross-border consistency, and because the validity of the Bosscheveld formation has been questioned (Vis et al., 2025), the interval between 456 and 500 m depth is allocated to the Condroz Formation. The interval between 456 and 397 m is now allocated to the Hastière formation (Figure 12). The resulting stratigraphic profile deviates from the original profile (Figure 12). Mozafari et al. (2019) suggested a stratigraphic amendment after recognising elevated gamma-ray levels associated with the Pont d'Arcole formation (Figure 12). Here,

https://doi.org/10.70712/NJG.v105.12991

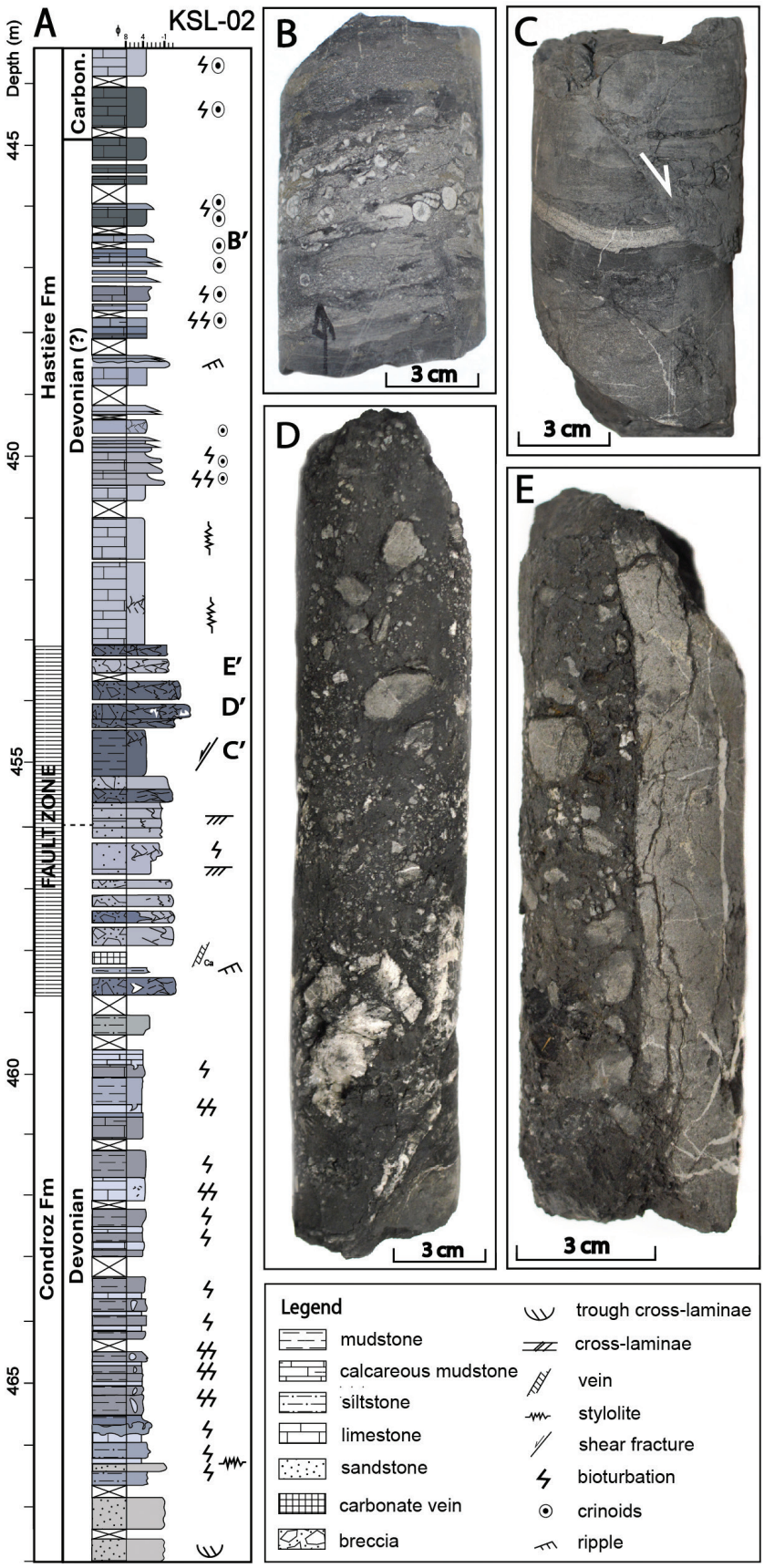

Figure 11. (A) Sedimentary log of Kastanjelaan-02. (B) Core piece showing crinoidal-rich carbonate at 446.5 m. (C) Shear fracture at 454.4 m. (D) Cross-laminated fine micaceous sandstone at 468 m. (E) Paleokarstic structures at 465.4 m. (F) Chaotic breccia at 453.4 m. (G) Chaotic breccia with carbonate vein fragment at 454 m. Note the lithofacies change above and below the fault zone in A.

https://doi.org/10.70712/NJG.v105.12991

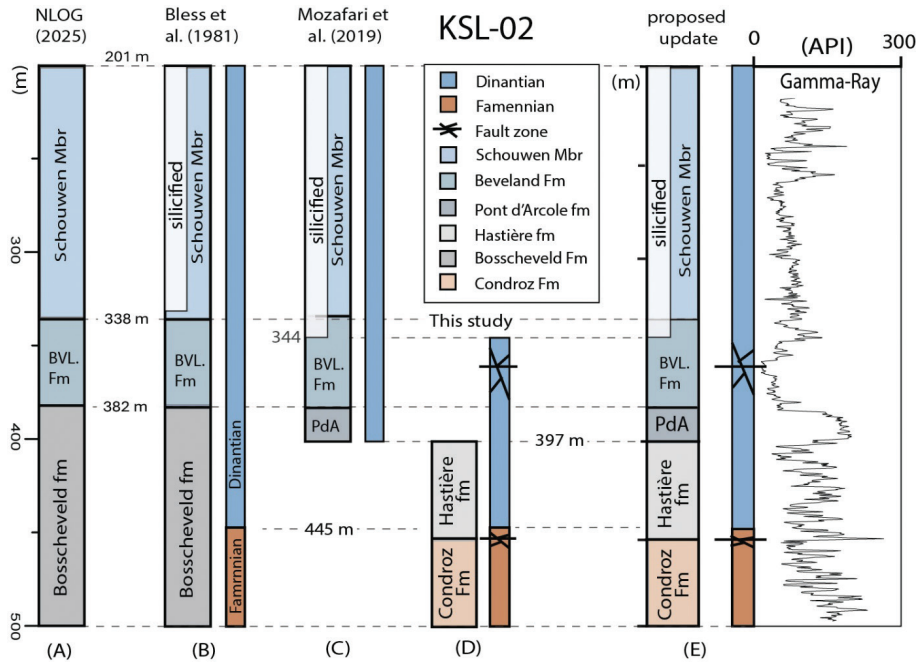

Figure 12. Different stratigraphic profiles of the Paleozoic succession in KSL-02, dotted lines indicate depths of stratigraphic boundaries. The left columns are lithostratigraphic interpretations, and the right are chronostratigraphic interpretations. (A) Lithostratigraphy after geodatabase viewer (NLOG, 2025). (B) Profile by Bless et al. (1981a) (C) Suggested stratigraphy by Mozafari et al. (2019). (D) Stratigraphic profile with faults indicated as interpreted in this study. (E) Suggestion for an updated profile. BVL = Beveland mbr, PdA = Pont d'Arcole formation.

we update the original description with the amendments suggested by Mozafari et al. (2019) and this study (Figure 12), while adhering to an updated nomenclature (Mottequin et al., 2024; Vis et al., 2025). The resulting stratigraphic profile deviates from the NLOG geodatabase viewer (2025; Figure 12).

RWTH-1

Borehole RWTH-1 was drilled near the campus of RWTH Aachen University in 2004 for geothermal exploitation. The borehole is 2544.50 m deep and Paleozoic strata were reached after drilling 20 m (Ribbert, 2006). Three intervals from 1392–1516 m, 2128–2143 m, and 2537–2545 m were cored and well-log data, such as a dip meter log and a gamma-ray log, were acquired. Below a depth of 1263 m, acoustic and electric resistivity image logs were also acquired. These well-log data were analysed to study the in situ crustal stress state (Trautwein-Bruns et al., 2010) and for its structural setting (Trautwein-Bruns et al., 2011).

Deviating stratigraphic profiles of the RWTH-1 borehole exist (Figure 13). The original description of cuttings and cores describes a thick siliciclastic succession (20–1025 m) corresponding to Namurian-A (Ribbert, 2006). Other stratigraphic profiles suggest that the succession is of both Namurian and Westphalian-A in age (Figure 13), without indication of the boundary between them (Becker et al., 2011; Trautwein-Bruns et al., 2011). Based on new palynological data (Supplement, S3.5), the interval from 20 to 40 m is interpreted as Westphalian, and the interval 300–780 m as Namurian-A (TK-Zone; Clayton et al., 1978). These results contrast with the original borehole description and constrain the depth of the Namurian-Westphalian boundary somewhere between 40 and 300 m (Figure 13). Faults are annotated differently among the existing stratigraphic profiles (Figure 13). For example, Sindern et al. (2008) indicate a fault contact at 1440 m, while Becker et al. (2011) indicate a hiatus at this depth (Figure 13). This contact at 1440 m is cored and characterised by numerous quartz-carbonate-chlorite veins (Becker et al., 2011; Sindern et al., 2008, 2012). Veins frequently exhibit slickensides with steps indicating both up- and down-dip slip. Pseudotachylite and fault breccias testify to high stresses (Sindern et al., 2012). The paleofluid composition of veins from the same interval was interpreted as being introduced from a Variscan brine along a fault (Sindern et al., 2012). On top of that, the scattered bedding attitude and sudden dip change indicate deformation around 1440 m (Figure 14), and the increased fracture density suggests a fault zone (Pechnig, 2005). Based on dip patterns and shear wave velocity anisotropy, Trautwein-Bruns et al. (2011) also indicated a zone of high deformation exceeding a width of 150 m and interpreted as a thrust zone from 1269 to 1437 m (Figure 13). These observations collectively suggest that the contact between the Lower Devonian and the Famennian is most likely a fault contact, rather than a hiatus.

Inspected borehole reports

Mezzel-6 (DB-141), Baneheide (DB-115), and Horbach VI

Inconsistencies were identified between stratigraphic profiles in borehole reports and geodatabase viewers. The Mezzel-6 (DB-141) borehole was drilled only 285 m apart from the recent Cottessen borehole. Its original description describes a micaceous sandstone succession from 32.25 m to the base at 186.92 m (Geologisch Bureau, 1937). These sandstones underlie mudstones and thus, have a similar lithostratigraphic succession as the Cottessen core (Section 4.3.1). Therefore, the mudstones (3.10–32.25 m) most likely represent the Epen Formation, and the micaceous sandstones (32.25–186.92 m) the Condroz Formation. However, on the

https://doi.org/10.70712/NJG.v105.12991

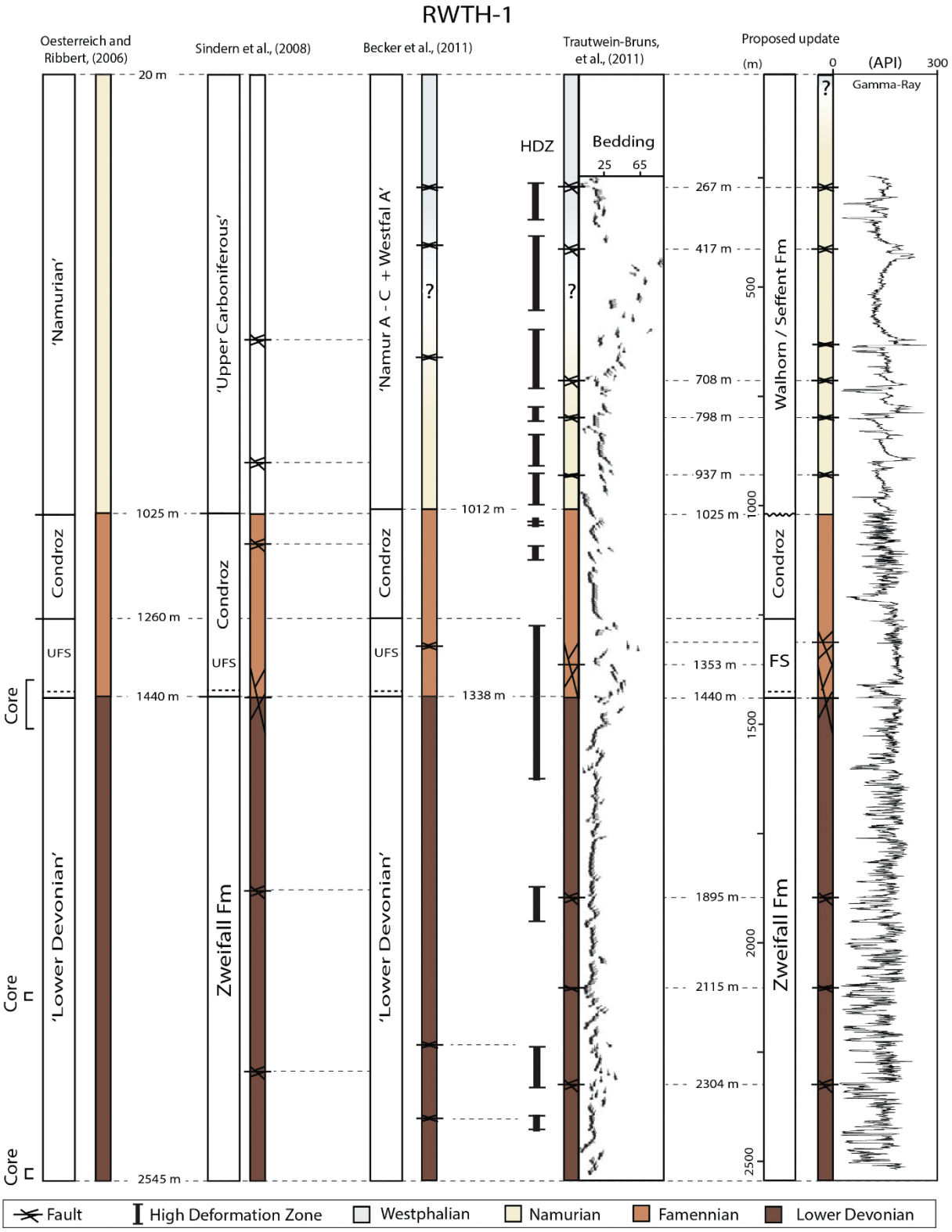

Figure 13. Different stratigraphic profiles of RWTH-1 with tadpoles and a gamma ray log from Trauwein-Bruns et al. (2011). Note the differences in fault zone locations. The profile on the right is a reinterpretation of this study. UFS = upper famenne shales; FS = Famenne shales.

NLOG geodatabase viewer, the upper Carboniferous Limburg Group is indicated for the entire borehole (NLOG, 2025). Thus, stratigraphic information from the geodatabase viewer mismatches a retrospective lithostratigraphic interpretation made with additional information.

Borehole Baneheide (DB-115) is a 509.65 m deep borehole (Figure 2), which reached Paleozoic strata below 130.50 m (Geologisch Bureau, 1985). Strata were initially interpreted as lower Westphalian, based on coal beds in the 307–400 m interval (Patijn & Kimpe, 1961). Later, however, index

https://doi.org/10.70712/NJG.v105.12991

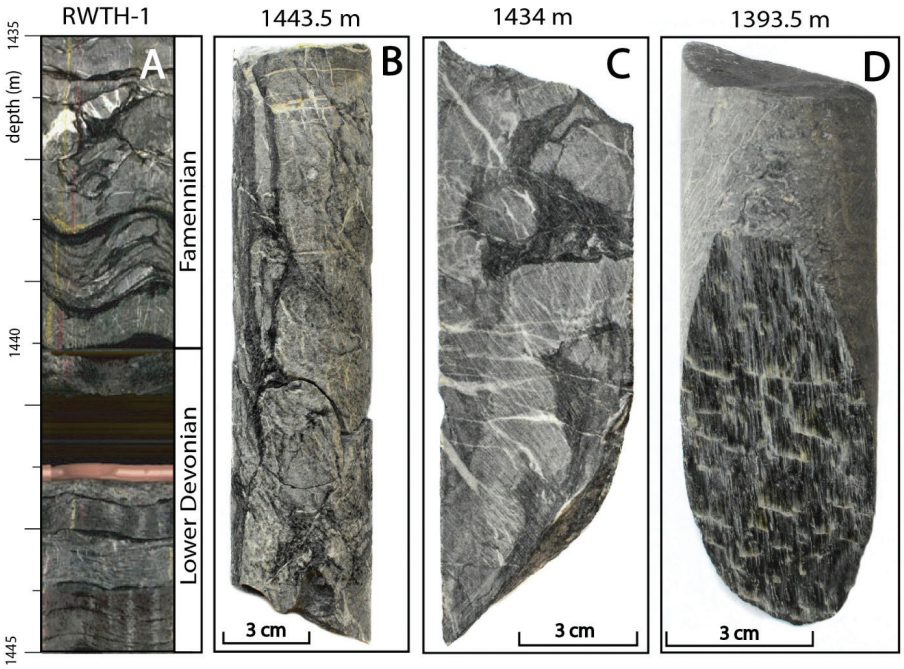

Figure 14. (A) Borehole image log televiewer of RWTH-1 at the Famennian-Lower Devonian contact around 1440 m (Trautwein-Bruns et al., 2011). (B) Deformed rock in the RWTH-1 core at 1443.5 m. (C) Fault breccia with juxtaposed sand and mudstone at 1434 m. (D) Chlorite slickenfibres indicating up dip-slip at 1393.5 m.

goniatites from the upper part were interpreted as being of Namurian age (Geologisch Bureau, 1985). The resulting age-conundrum was explained by interpreting a thrust fault that displaced Namurian strata over Westphalian-A strata (Geologisch Bureau, 1985). This fault was described with a ~270 m vertical throw located at 170 m depth (Geologisch Bureau, 1985). Yet, in the original report, this fault zone is described slightly deeper at 187.10–215.70 m (Geologisch Bureau, 1922). We incorporated the amendment of Geologisch Bureau (1985) while adhering to the original depth of the fault zone. The resulting stratigraphic profile deviates from the NLOG viewer (NLOG, 2025), indicating uncertainty in the geodatabase viewer.

Horbach VI is a 182 m deep borehole drilled in 1948 in the former Melanie mining concession (Figure 2), west of Kohlscheid (Germany). The borehole reached Carboniferous strata after drilling 21.4 m and encountered the Steinknipp marker bed indicating an early Westphalian age for the strata overlying this marker (Maurenbrecher, 1944). Although the abovementioned information is available in the physical archive of NRW, the Horbach VI borehole is not included in the NRW geodatabase viewer (Geobasis NRW, 2025). This lack of information exemplifies an uncertainty caused by limited data availability.

Lanaye boreholes (108W-202, 108W-203, 108W-204) and Eysden (DB-144)

Three boreholes (108W-202, 108W-203, 108W-204) were drilled at Lanaye (Belgium, Flanders; Figure 15A). The Paleozoic strata were all described as Namurian shales, based on their dark grey coloured shaley appearance. Later, however, microfossils were found in these strata that indicated a Dinantian age (Kimpe et al., 1978; Pirlet, 1967). Based on these age constraints, it was argued that the Lanaye boreholes encountered weathered and silicified Dinantian carbonates that resemble shales (Bless et al., 1976). This amendment is unmentioned in reports provided by the DOV geodatabase viewer for these boreholes (DOV, 2025). Thus, the Lanaye boreholes exemplify both uncertainty in geodatabase viewers and uncertainty caused by ambiguous lithofacies.

Similarly, Kimpe et al. (1978) argued that silicified shales in the Eijsden area suffered similar interpretation problems and are actually of Visean age. Yet, in the NLOG geodatabase viewer, the Paleozoic section of the Eysden borehole (DB-144) is indicated as the Namurian Epen Formation (NLOG, 2025). Thus, the NLOG geodatabase viewer mismatches the most recent stratigraphic constraints for the DB-144 borehole.

Evaluation of maps and structures

Based on the compiled borehole dataset (Figure 8), we assess the uncertainty of geologic maps and appended cross-sections, focusing on the most recent top-Paleozoic map (RGD, 1995). As highlighted before, we do not intend to critique these legacy materials, rather, we evaluate them to examine sources of uncertainty from a modern-day geomodelling perspective. We examine a subset of four geologic structures depicted on geologic maps (Bless et al., 1976; Kimpe et al., 1978; RGD, 1995) and trace their origin in legacy literature. To this end, the *Border Fault, Geul Fault, Visé-Puth Anticline, Waubach Anticline, and the Val Dieu anticline* were selected (Figure 2).

Geological maps and cross-sections

Comparing three geologic maps with borehole stratigraphy of the compiled dataset (Figure 1C) revealed several mismatches. A geologic map covering the Geul River-Valley (Laloux et al., 2000) conforms with our compiled dataset, and a Paleozoic subcrop map in the Belgian Visé region (Barchy & Marion, 2007) has one mismatch. The top-Paleozoic geologic map of South Limburg and surroundings (RGD, 1995) contains 22 mismatches (Figure 15A). Four mismatches are related to information in geodatabase viewers that was revised (Section 4.3.3). Most other mismatches are near stratigraphic

https://doi.org/10.70712/NJG.v105.12991

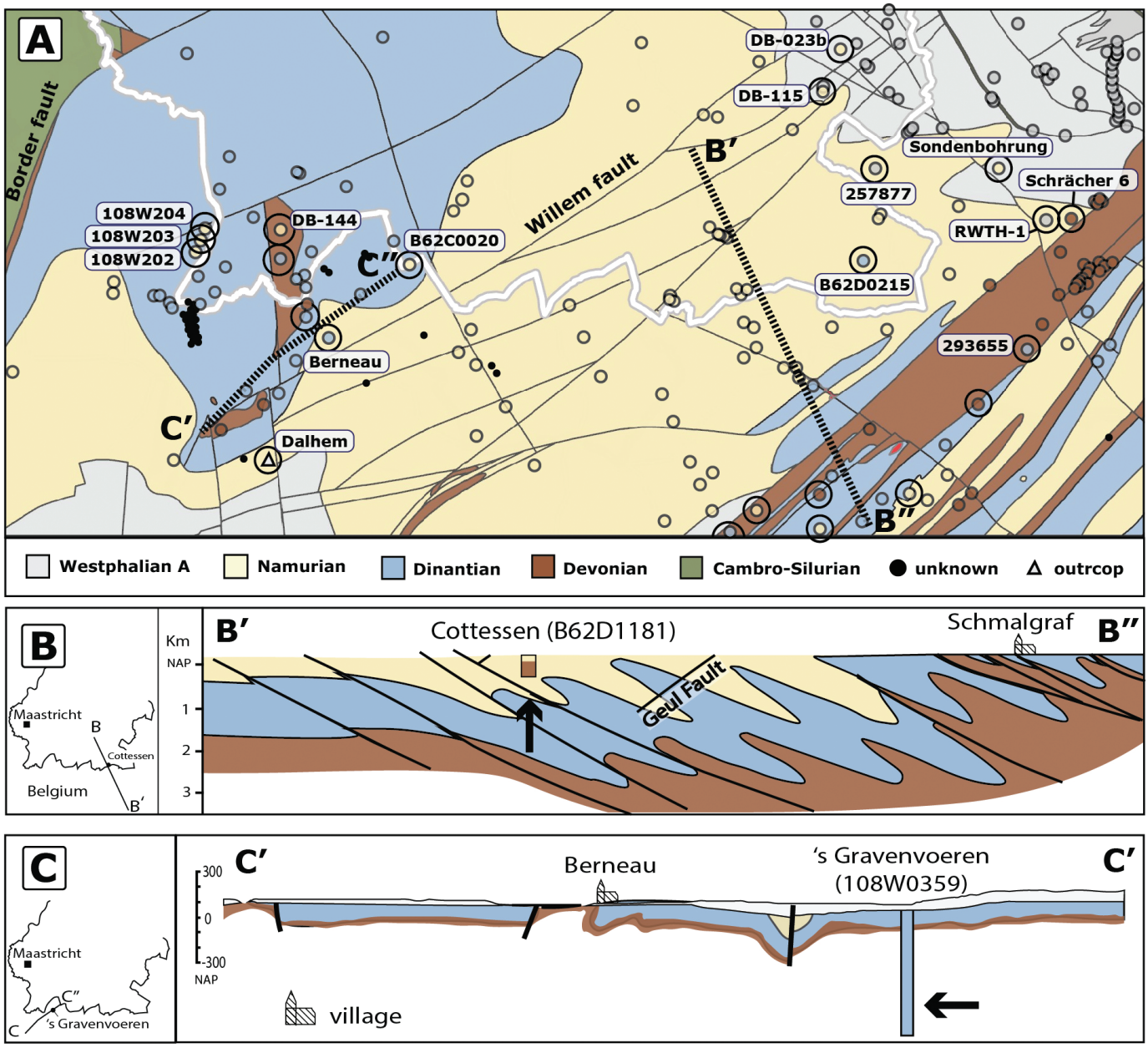

Figure 15. Geologic map and cross-sections with borehole stratigraphy overlain for comparison. (A) Southern part of the most recent top-Paleozoic map (RGD, 1995). Circles indicate mismatching stratigraphy. (B) Cross-section appending this map. (C) Cross-section appending geologic map sheet (34/7–8) covering Visé-St-Martens-Voeren (Barchy & Marion, 2007). Note the mismatches indicated by black arrows.

boundaries (Figure 15A), suggesting an uncertainty of limited magnitude. Nevertheless, the mismatches indicate that the RGD (1995) map should be used cautiously outside the coal mining region.

The recent cottessen-borehole revealed an unconformity whereby the Dinantian succession is completely missing (Figure 9D). This stratigraphic gap is not shown in the cross-section appending the RGD (1995) map (Figure 15A). The top-Famennian contact of the recently drilled Cottessen borehole also mismatches the cross-section with a depth difference of ~2 km (Figure 15B). Similarly, stratigraphy of the 's Gravenvoeren borehole shows a ~500 m mismatch with a cross-section through the Visé region (Barchy & Marion, 2007; Figure 15C). These mismatches indicate that these cross-sections are a source of uncertainty for geomodelling.

Faults

Numerous faults are depicted on the RGD (1995) map (Figure 2). Of these faults, we discuss the *Geul Fault* and the *Border Fault*. Along the Geul valley, the *Geul Fault* is indicated on the RGD (1995) map (Figure 2). Outcrops in Plombières expose two NW-SE oriented slickensides (170°, 77°) with sinistral strike-slip indicating steps. We measured similarly oriented slickensides at the Cottessen quarry (148°, 35°) along the trajectory of the *Geul Fault*. Oblique sinistral indicating slickenfibres on a vertical plane (strike = 132°) are also present in the Cottessen core at 195.5 m depth. Furthermore, the *Geul Fault* trajectory coincides with Pb-Zn mineralisations (RGD, 1995), including the fault-related Sippenaeken and Plombières deposits (Dejonghe, 1998; Geologisch Bureau, 1954). A borehole report

https://doi.org/10.70712/NJG.v105.12991

from an inclined well in Plombières (Belgium; Bl-2) describes a transfer fault at 342 m coinciding with the *Geul Fault* (Wallonie, 2025). These observations support the existence of the *Geul Fault* as depicted on the map (RGD, 1995) and, despite few kinematic indicators (n = 4), it possibly has a sinistral strike-slip component.

The *Border Fault* is depicted on the RGD (1995) geologic map with a SSW-NNE strike running through South Limburg including the city of Maastricht (Figure 2A). On an older map (Bless et al., 1976), this region was left blank and the border fault was indicated with a question mark. In the 1970s, in an attempt to constrain the location of the *Border Fault* north of Liège, five nearby boreholes were drilled near Viller-Saint-Siméon (Legrand, 1977). At this location in Belgium the strike of the fault can be inferred from gravity data (Bless et al., 1980; Everaerts & De Vos, 2012) and it was extrapolated towards Maastricht in the NNE (Figure 2). Only a few boreholes are located NNE of Villers-Saint-Simeon (Figure 8), making this extrapolation uncertain. The *Border Fault* is depicted on the RGD (1995) map, continuing in South Limburg to connect with the so-called *70 m Fault* (Figure 2). No evidence was found in this data review that suggests a connection between the *Border Fault* and the *70 m Fault*. Both the orientation and kinematics of the *Border Fault* differ from the *70 m Fault* (Legrand, 1977; Sax, 1946; Figure 2). Therefore, connecting these two faults, as depicted on the RGD (1995) map, is somewhat speculative.

Anticlines

Three anticlines are reviewed of which two are shown on the RGD (1995) map named *Visé-Puth Anticline* and *Waubach Anticline*. The *Waubach Anticline* is described with elevated Cl and Pb-Zn concentrations in groundwater (Kimpe, 1963; Kimpe et al., 1978). The anticline is inferred from the shallow sub-cropping of the Namurian amid Westphalian deposits and is depicted on Dutch maps (Kimpe et al., 1978; RGD, 1995) with a SW-NE trending axis (Figure 2). This orientation suggests a genetic link with Variscan deformation (Patijn, 1963b). Towards the east, in the Aachen coalfield, the Waubach anticline is depicted with a NNE-SSW orientation (Wrede & Zeller, 1988). This variation could be explained by the curvature of the Variscan fold-and-thrust belt around the London-Brabant-Massif (Wrede & Zeller, 1988).

The *Waubach Anticline* is described as a SW-plunging anticline with the northern flank running until the *10 m Fault* (Sax, 1946). Later, a seismic survey in the Voerendaal area (South Limburg) suggested the existence of the *Anticlinal Fault* (Patijn & Kimpe, 1961). Afterwards, the *Waubach Anticline* was associated with this nearby *Anticlinal Fault* and ran until this fault on top-Paleozoic maps (Kimpe et al., 1978; RGD, 1995; Figure 2). Furthermore, the *Waubach Anticline* is described as an asymmetric anticline with a gently dipping southern and a steeper dipping northern flank (Sax, 1946). This vergence, and its association now with the *Anticlinal Fault*, is characteristic of a hanging wall anticline (Fossen, 2016). Legacy cross-sections also show the *Willem Fault* with a hanging wall anticline geometry (Figure 4E). Likewise, the *Waubach Anticline* can be interpreted as a hanging wall anticline of the *Anticlinal Fault* (Figure 4E).

The *Puth Anticline* (Figure 2) was recognised in the Maurits mine and interpreted as compression flexure (Dikkers, 1945; Patijn, 1963a; Sax, 1946). This *Puth Anticline* is expressed as Namurian strata amid Westphalian strata near the village of Puth (Kimpe et al., 1978). The *Puth Anticline* occurs along strike the *Visé Anticline* and was interpolated as a single structure, named *Visé-Puth Anticline*, on the Dinantian depth contour map (Bless et al., 1976). The *Visé-Puth Anticline* corresponds to enhanced Cl-concentrations in soils and mining waters (Bless et al., 1976; Kimpe et al., 1978) and a -5 mGal negative gravity anomaly (Bless et al., 1981b). Frasnian exposures, at Souvré and La Folie (Section 4.2.2) were interpreted as the core of the *Visé Anticline* (Bless et al., 1976).

The unconformity at the Frasnian-Dinantian contact at the La Folie quarry (Figure 2; Section 4.2.2) led Bless et al. (1976) to interpret the *Visé Anticline* as a synsedimentary ridge. In addition, the *Puth Anticline* was interpreted to have affected Westphalian sedimentation (Bless, 1973), ultimately leading Bless et al. (1976) to interpret that 'the anticline has been a synsedimentary ridge from at least the Dinantian to lower Westphalian times and was at least intermittently active'. This interpretation assumes that the *Visé-Puth Anticline* was already one joint structure during the Dinantian. Deformed Westphalian strata as part of the *Puth Anticline* (Dikkers, 1945) imply that the *Puth anticline* formed or deformed during or after Westphalian times. Thus, if the *Visé* and *Puth Anticlines* are part of a single connected structure, the cross-cutting relationship suggests it formed either by progressive or multi-phase deformation up to Westphalian times. Although the connection of the two anticlines has not been confirmed by additional data and few boreholes are located between the two structures (Figure 8).

The *Val Dieu Anticline* is expressed by a southwest-northeast oriented band of Famennian strata outcropping amid Namurian strata (Barchy & Marion, 2000). The anticline is interpreted as a structure in the hanging wall of a Variscan thrust fault (Ancion et al., 1943; Barchy & Marion, 2000). The structure was first described based on field data near the abbey of Val Dieu and a former quarry named Booze (Ancion et al., 1943). The exposed strata revealed an unconformable contact between Famennian and Namurian strata (Ancion et al., 1943; Graulich, 1955). This unconformity is interpreted as formed by a structural high, named *Booze-Le Val-Dieu Ridge*, which has been extrapolated from Val Dieu to the northeast towards Aachen (Arndt et al., 2020). This paleogeographic feature is considered to have separated different basins or acted as a shoal during the Dinantian (Bless et al., 1980a, 1980b), and was later deformed by Variscan tectonics (Graulich, 1955).

In the recently drilled Cottessen and Terziet boreholes, an unconformity between Famennian and Namurian strata was also found (Figure 9D). These boreholes are located in the southwest-northeast continuation of the mapped *Val Dieu Anticline* (Figures 1, 2). Assuming the unconformity in Cottessen and Terziet is part of the same structure, these new data confirm the previously interpreted trend of the *Val Dieu Anticline* and demonstrate a degree of certainty in legacy concepts.

Identifying uncertainties

In statistics, a distinction is made between quantitative uncertainty that is described numerically and qualitative uncertainty that can be described categorically (Bulmer, 2012; Funtowicz & Ravetz, 1990). Quantitative uncertainties are somewhat similar to precision and are described by

https://doi.org/10.70712/NJG.v105.12991

statistical probability using uncertainty ranges. In geomodelling, this uncertainty can, for example, describe the uncertainty range of a predicted fault strike (e.g. 45–65˚), regardless of whether the fault actually exists. In contrast, qualitative uncertainties relate to interpreting non-numerical data and are more akin to accuracy. They are expressed in terms of probable or improbable. Qualitative uncertainty can describe the probability of whether a fault exists at all. Such uncertainties can be expressed by an estimated number to incorporate them into a Bayesian modelling framework (Joo et al., 2020). Estimation, however, can be challenging and requires an understanding of these uncertainties. Here, we reflect on the encountered uncertainties in geomodelling inputs and group them into different types (Table 2).

Uncertainty scheme

An uncertainty scheme was made specifically for geologic mapping (Mann et al., 1993), which was later adapted in the context of geomodelling (Wellmann et al., 2010). In the latter scheme, three uncertainty types were categorised relating to (1) data imprecision and quality, (2) stochasticity and geostatistical interpolations, and (3) incomplete knowledge about the geological domain (Wellmann et al., 2010). However, as exemplified in this article, an incomplete knowledge of the geological domain (Type 3) can manifest itself in input materials (Type 1). This overlap invites a closer look at input-related uncertainties to find their causes, which helps with more effective tracking of uncertainty. Therefore, causes of uncertainty are identified and comprehensively classified (Table 2). The presented categories affect the making of an explicit static model, made from cross-sections (Lemon & Jones, 2003) also called a geometric or framework model (Wood & Kessler, 2021). The following sections elaborate on the types of uncertainty listed in Table 2.

Uncertainty in stratigraphic interpretation

Uncertainty in stratigraphy interpretation (Type a) is caused by observational limitations and ambiguity (Figure 16). This is exemplified by the weathered Dinantian carbonates resembling Namurian shales (Section 4.3.3). This resemblance caused interpretation problems resolved with additional biostratigraphic constraints (Bless et al., 1976; Kimpe et al., 1978). Similarly, diagenetically formed breccias can be ambiguously interpeted as breccias formed by tectonic processes (Flude et al., 2025). This ambiguity results in multiple viable stratigraphic interpretations, causing uncertainty (Høyer et al., 2024).

Uncertainty in biostratigrpahic interpretation originates from (1) limitations of identification, (2) contamination and reworking, and (3) an imprecise calibration. The first source of uncertainty is demonstrated by samples of the Banholt borehole (Section 4.3.1). Microfossils were altered to an extent that no interpretation could be made by specialists (Section 4.3.2). Ultimately, no distinction between a Namurian or Westphalian age was possible (Section 4.3.1). Uncertainty caused by the possibility of reworking is exemplified by trying to pinpoint the Devonian-Carboniferous boundary in the Kastanjelaan borehole (Section 4.3.2). Due to reworking, microfossils can indicate an older age than its host rock. This possibility of reworking causes quantitative uncertainty on the precise depth of a stratigraphic contact.

Uncertainty in fault interpretation

Uncertainty in interpreting faults (type b) is caused by problems with their recognition and interpreting their scale. Difficulties with recognising faults are exemplified by differences in fault interpretation between borehole profiles of Kastanjelaan-2 and RWTH-1 (Figures 12 and 13). Faults in boreholes are often not discrete planes but rather zones of fractured strata. Fracturation, however, can also be caused artificially during drilling, which makes it challenging to determine its cause. A means to recognise if the fractured interval is a fault zone is the presence of breccias (Figure 11D, E). However, breccias can form in seven different environments by different processes (Flude et al., 2025), thereby complicating their interpretation. Specific features, such as a piece of broken-up mineral vein as clasts (Figure 11D), can help to discriminate between different breccias. Two other features associated with fault zones is the juxtaposition of stratigraphic units and dragged bedding patterns (Figure 11A). The stratigraphic order of the juxtaposed units and the bedding patterns help to discriminate between normal and thrust faults (Fossen, 2016). Furthermore, recognising faults is also aided by borehole image logs. These logs help to recognise increased fracture density and bedding patterns around fault zones (Section 4.3.1). However, we

Table 2. Categories of uncertainty recognised in geomodelling-inputs in this study.

Type of uncertainty	Causes	Example
a. Stratigraphic interpretation	-Ambiguity of interpreting data	Resemblance of Namurian mudstones and weathered Dinantian silicified strata
	-Indiscernible fossils	
	-Possibility of reworking of fossils	
b. Fault interpretation	-Problems in scaling fault dimensions	Deciding to incorporate a fault with ~25 m damage zone into a regional cross-section
	-Interpreting damage zone thickness	
	-Lacking stratigraphic constraints	
c. Transferring data	-Differences in presented information	Differences in indicated bore-hole stratigraphy and faults among different sources
	-Consequences of stratigraphic revision	
d. Legacy materials	-Inconsistencies in interpretive products	Geologic cross-sections or maps that mismatch borehole stratigraphy

The letters a–d are used in Figure 16 and Table S5.1.

https://doi.org/10.70712/NJG.v105.12991

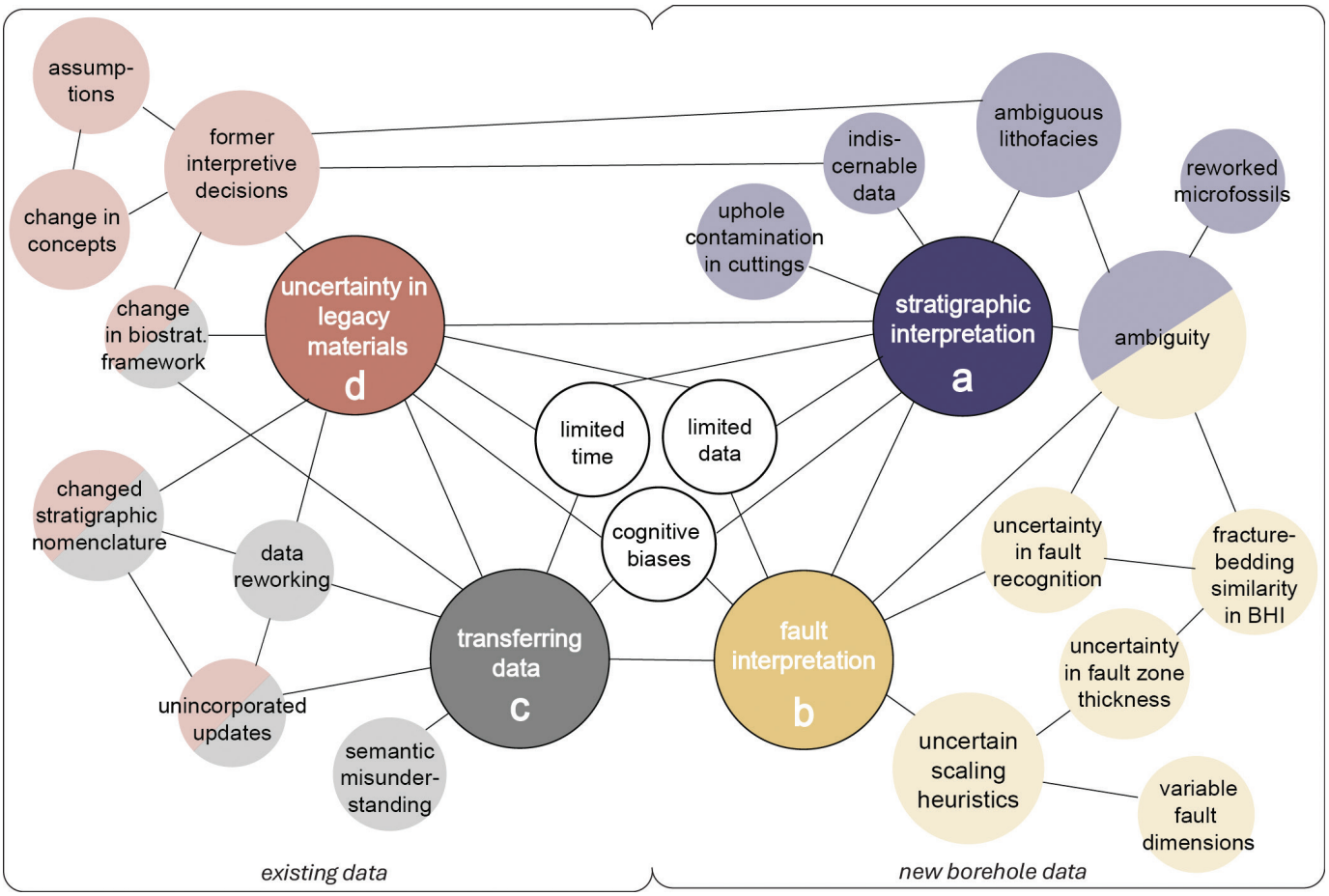

Figure 16. Sources of uncertainty recognised in geomodelling inputs for explicit modelling of the architecture of deformed domains. Letters a–d refer to Table 1. Uncertainties in geophysical survey data are excluded. The network shows numerous intertwined sources that challenge an overview of all the uncertainties accumulated in the process. The term ***ambiguity*** refers to how data can be interpreted in more than one equiprobable way. Definitions for each term are provided in Supplement Table S5.1.

demonstrated a resemblance between similarly oriented bedding and fracture planes that caused errors in interpreting image logs. Despite this pitfall, borehole image logs are still helpful tools in recognising fault zones, as demonstrated with the case of the Banholt and Cottessen boreholes (Section 4.3.1).

Besides difficulties in recognising faults, uncertainty in interpreting them (type b) is caused by interpreting their scale. Determining the offset of faults when making cross-sections introduces uncertainty (Figure 16). The damage zone thickness is taken into consideration when interpreting the offset of faults by scaling laws (Torabi & Berg, 2011). However, problems can arise when pinpointing the outer limit of a damage zone, and deviating criteria are used in practice and literature (Torabi et al., 2020). In the example of the Banholt borehole, the thickness could not be determined as drilling stopped in the fault zone (Section 4.3.1). In addition, faults in boreholes have apparent thicknesses due to the trigonometric relationship between a dipping fault zone and a vertical hole. Hence, if the dip of the fault is unknown, the actual fault thickness cannot be determined precisely, challenging the interpretation of the scale of a fault by scaling laws.

When the damage zone is known, uncertainty persists as damage zone thickness varies along its fault plane (Caine et al., 1996). Empirical relationships between fault dimensions and fault zone thickness suffer from substantial natural variability (Sperrevik et al., 2002; Torabi & Berg, 2011). Therefore, scaling heuristics – a thicker fault zone has a larger offset – serve as a rough estimator, which does not necessarily hold true. Because of the scaling problems, deciding to incorporate a fault into a regional cross-section comes with uncertainty. This qualitative uncertainty affects the boundary conditions of geomodels and can be handled by scenario-based modelling.

Uncertainty in transferring data

Uncertainty in transferring data (Type c) can arise from inconsistencies in data communication as processed data are shared among peers. These uncertainties affect the position of stratigraphic bounding surfaces and thereby the geometry of the geomodel. Uncertainty in data transfer is exemplified by stratigraphic borehole profiles of the same borehole that differ among various sources (Section 4.3.2). These differences can result from revised stratigraphic nomenclature (Mascarelli, 2009), as for the Kastanjelaan-02 borehole (Section 4.3.2). Differences in presented information were also observed in seven examples of borehole reports deviating from stratigraphic profiles by geodatabase viewers. These inconsistencies arise from revised stratigraphic interpretations that are not updated in geodatabase viewers or

https://doi.org/10.70712/NJG.v105.12991

with a delay. These inconsistencies are hard to tackle given the size of geodatabases and the accumulation of data and insights.

Uncertainties arising from transferring data in geoscience have also been found to relate to semantic misunderstanding and data reworking (Ma et al., 2014). Semantic misunderstanding occurs when processed data are understood differently than intended by the provider. As processed data are passed on to coworkers or peers, a data reworking can occur and errors can propagate that are easily unnoticed in cross-disciplinary geoscience projects (Allen et al., 2008; Ma et al., 2014).

Uncertainty in legacy materials

Uncertainty in legacy materials (type d) can be caused by changing paradigms and concepts after new data were acquired. This uncertainty was revealed as mismatches with the data (Figure 16). For example, the geologic map discussed in Section 5 (RGD, 1995), is demonstrated to have mismatches with borehole data (Figure 15A). Also, cross-sections may mismatch borehole stratigraphy by 100-1500 m (Figure 15B, C). These mismatches indicate qualitative uncertainty from interpretive decisions made to complete the geologic map and cross-sections. Due to these interpretive decisions, geologic maps always have some degree of qualitative uncertainty. However, two other geological maps in Belgium conform to the dataset, which demonstrates a degree of certainty in the legacy materials.

Geologic concepts that changed over time can cause misconceptions in legacy materials. This is exemplified by a coal mining cross-section made before the 1960s showing mechanically unfavourable geometries (Section 5.1). This is because older coal mining sections were drawn with different geologic principles of tectonic processes of times before plate tectonics gradually became widely accepted (Nitecki et al., 1978). Misconception arises when the underlying assumptions in legacy interpretation are now understood differently. Nevertheless, mining cross-sections also show mechanically realistic geometries that provide helpful information (Section 5.1). Assessing structural interpretations in coal mining cross-sections helps to examine whether faults have mechanically favourable angles and offsets and look whether geometries are similar to natural examples (Section 5.1). The degree of consistency of structural style within a concession can also guide an assessment. Uncertainty in maps and cross-sections can be assessed by comparing them with the data itself. However, this validation process can be challenging as mine shafts are closed and former outcrops are sometimes inaccessible or partly overgrown (Section 4.2). Yet, a swift validation check can already provide a useful estimation of uncertainty.

Cognitive bias

Where data are inconclusive, interpretative decisions are made that, albeit logical, suffer from unconscious cognitive biases (Baddeley et al., 2004). For example, when several equally probable interpretations can be derived from the data, a person is often inclined to favour the option that best fits his or her conceptual model, i.e. *confirmation bias*. When working in a group, a person can be inclined to interpret what is generally accepted, referred to as the *bandwagon effect* (Polsen & Curtis, 2010). A cognitive bias can also occur when a person tends to overly rely on the first piece of data or information that he or she comes across (Tversky & Kahneman, 1974). Similarly, a person can overly rely on prior knowledge related to experience, known as *availability bias* (Tversky & Kahneman, 1973). These cognitive biases can influence interpretation across all identified types (Figure 16). Yet, despite these cognitive biases, geological interpretation is factual and based on objective criteria (e.g. see Section 6.1.2). To ensure these impartial interpretations, it can be necessary to use working hypotheses (Chamberlin, 1965) or working with scenarios when making maps or cross-sections (Bentley & Smith, 2008).

Towards weighing uncertainty

Tracking uncertainties that enter the geomodelling process is challenged by numerous intricate links between various causes (Figure 16). The main categories of uncertainty are linked, obscuring the boundaries between categories. For example, uncertainty in legacy materials (type d) affects uncertainty in transferring data (type c). Also, uncertainty in stratigraphic interpretation affects the fault interpretation if different stratigraphic units are juxtaposed. Additionally, all uncertainty types are affected by an interplay of limited data, limited time, and cognitive biases (Figure 16). These interconnections imply complexity that adds up in the uncertainty chain of geomodelling.

The identified causes and uncertainty scheme (Table 2) allow to gain a better understanding of uncertainty in geomodelling inputs. Yet, the question of how often each uncertainty arises remains an open question. In the investigated case, uncertainty caused by interpreting stratigraphy was recognised repeatedly. Yet, the frequency of uncertainties can be irrelevant if an uncertainty has little effect on model outcomes. Therefore, the magnitude of each uncertainty is a most relevant subject for further research. For example, the quantitative effect of uncertainty in transferring data (type c) on geological models can be examined by numerical sensitivity tests. Alternatively, a qualitative criterion can be used to compare their weights. For example, discriminating whether the uncertainty is quantitative or qualitative can be helpful to rank them. Qualitative uncertainties can substantially change the boundary conditions and is, therefore expected to have more impact than quantitative uncertainties.

Most stratigraphic mismatches between borehole data and the studied geologic map (RGD, 1995) are near stratigraphic boundaries (Figure 15). These mismatches therefore suggest uncertainty that has a limited impact on model outcomes. On the contrary, cross-sections (Barchy & Marion, 2007; RGD, 1995) have depth mismatches up to 1500 meters (Figure 15). These mismatches have substantial impacts on the model boundary conditions and thus outcomes. To better understand the relevance of these uncertainties, future research could contribute by testing and comparing the magnitude of uncertainties to ultimately make a ranking and prioritisation for different subsurface cases. Sensitivity analyses are used to study the effect of uncertainty in stratigraphic interpretation (Liu & Wang, 2022). Similarly, the impact of uncertain scaling of faults can be examined by sensitivity testing and then compared with test results examining uncertainty related to transferring data. Eventually, each uncertainty can be incorporated into the modelling workflow using a Bayesian method (De la Varga & Wellmann, 2016). When geological uncertainty involves substantial qualitative uncertainty,

https://doi.org/10.70712/NJG.v105.12991

working with scenarios helps to describe uncertainty (Bentley & Smith, 2008). A better understanding of the magnitude of cascading uncertainties will ultimately lead to improved geomodels and better decision-making. This will aid the construction of a reliable geomodel and decision-making in subsurface engineering projects.

Conclusions

Our research objective was to identify causes of uncertainty in geomodelling input after compiling and reviewing subsurface data. These data review show the necessity of validating legacy materials to design a reliable modelling strategy before starting geomodelling. A vast amount of legacy knowledge and data exist and new data have brought new insights to this information. New litho- and palynostratigraphic results reveal an unconformity at the Famennian-Namurian contact in the Cottessen and Terziet boreholes. These new findings are in line with the *Val-Dieu Anticline* and *Booze-Le Val Dieu Ridge* described in legacy literature, demonstrating a degree of certainty. Reviewing data also revealed inconsistencies between (1) original borehole descriptions and stratigraphic information provided by online geodatabase viewers, (2) interpreted borehole image logs and cores, (3) borehole data and cross-sections, and (4) the compiled borehole dataset and two geologic maps. The examination of these inconsistencies suggests that causes of uncertainty are interconnected, thereby creating complexity. We identified various sources of uncertainty and categorised them into four main types. After this recognition, we call to investigate the magnitude of each uncertainty on model outcomes by sensitivity testing. The recognised uncertainties should eventually be incorporated into the modelling workflow. We draw the following conclusions:

1) Uncertainty in stratigraphic interpretations (type a) is caused by the ambiguity of lithofacies. This uncertainty is exemplified by a lithofacies of silicified Dinantian carbonates that are, in appearance, indistinguishable from Namurian mudstones. This type of uncertainty can permeate into geologic maps
2) Uncertainty in interpreting faults (type b) is caused by difficulties in their recognition and uncertainty in using scaling laws to estimate offsets of faults. This uncertainty permeates into geological cross-sections.
3) Borehole image logs demonstrated usefulness in recognising and interpreting faults; however, ambiguity in similarly oriented fractures and bedding planes challenges fracture identification.
4) Uncertainty related to transferring data (type c) is caused by stratigraphic reinterpretations of borehole reports that are not incorporated in geodatabases. This uncertainty is exemplified by stratigraphic profiles of the same borehole that are presented differently among various sources, i.e. literature and geodatabase viewers. Inconsistencies were found in this study for the following boreholes: Kastanjelaan-02, RWTH-1, DB-141, DB-115, and DB-144.
5) Uncertainty in legacy materials (type d), such as geologic maps and cross-sections, is caused by changes in paradigms and concepts from later insights. This uncertainty is exemplified in our case study by cross-sections that mismatch borehole stratigraphy up to 1500 meters. Two geological maps are also found to mismatch data to some degree, while one map conforms to the compiled dataset. Uncertainty in cross-sections can have a substantial impact on geomodel design.

Acknowledgements

This publication is part of the Dutch Black Hole Consortium with project number NWA.1292.19.202 of the research programme NWA, which is financed by the Dutch Research Council (NWO). This research would not have been possible without the advice of peers and colleagues from TNO – Geological Survey of the Netherlands. In particular, the authors would like to thank Bram Hoogendoorn for endlessly providing borehole reports and Jenny Hettelaar for helping with GIS software issues. In addition, they also thank Mariana Pinheiro for helping during her internship and Jan Kees Blom for advice, Erwin van Wingerden for providing support on the digital elevation model and Erik van Linden for sharing legacy data. The authors express their gratitude to Andrzej Slupik for hosting them in the core repository of TNO – Geological Survey of the Netherlands and Sascha Sandmann and Stephan Becker for help during visits to the Geological Survey of NRW. Finally, they thank the E-TEST and Einstein Telescope Euregion Meuse-Rhine (ET-EMR) projects for providing data and Bjorn Vink for his help.

References

Allen, D.M., Schuurman, N., Deshpande, A. & Scibek, J., 2008. Data integration and standardization in cross-border hydrogeological studies: a novel approach to hydrostratigraphic model development. Environmental Geology **53**: 1441–1453. DOI: 10.1007/s00254-007-0753-3

Amann, F., Bonsignorio, F., Bulik, T., Bulten, H.J., Cuccuru, S., Dassargues, A., DeSalvo, R., Fenyvesi, E., Fidecaro, F., Fiori, I. & Giunchi, C., 2020. Site-selection criteria for the Einstein Telescope. Review of Scientific Instruments **91**(9): 9. DOI: 10.1063/5.0018414

Ancion, C., Van Leckwijck, W. & Ubaghs, G., 1943. A propos de la bordure méridionale du Syncinal de Liège: la ride famenienne de Booze – Le Val-Dieu, à la limite septentrionale du plateau de Herve. Annales de la Société géologique de Belgique **66**: 229–335.

Aretz, M., Herbig, H.G., Wang, X.D., Gradstein, F.M., Agterberg, F.P. & Ogg, J.G., 2020. The Carboniferous period. *In*: Geologic time scale 2020 (pp. 811–874). Elsevier, Amsterdam.

Arndt, M., Fritschle, T., Salamon, M. & Thiel, A., 2020. Das Rhenoherzynische Becken – ein hydrothermales Reservoir für NRW und Nordwesteuropa? Scriptumononline -Geowissenschaftliche Arbeitsergebnisse aus Nordrhein-Westfalen. Geologischer Dienst NRW (Krefeld) **16**: 1–11.

Baddeley, M.C., Curtis, A. & Wood, R., 2004. An introduction to prior information derived from probabilistic judgements: elicitation of knowledge, cognitive bias and herding. Geological Society **239**(1): 15–27. DOI: 10.1144/GSL.SP.2004.239.01.02

Barchy, L. & Marion, J.M., 2000. Dalhem-Herve. Carte géologique de Wallonie à l'échelle 1: 25.000. 42/3-4. Notice explicative. Carte géologique de Wallonie à l'échelle 1: 25.000. Notice explicative. N° 42/3-4.

Barchy, L. & Marion, J.M., 2007. Visé-Sint-Martens Namur: Service Public De Wallonie. Voeren. Carte géologique de Wallonieà l'échelle 1/25.000. 34/7-8. Carte géologique de Wallonie à l'échelle 1: 25.000. Visé-st-Martins-Voeren 34/7-8. https://orbi.uliege.be/handle/2268/82913

Becker, G., Bless, M.J., Streel, M. & Thorez, J., 1974. Palynology and ostracode distribution in the Upper Devonian and basal Dinantian of Belgium and their dependence on sedimentary facies. Mededelingen-Rijks Geologische Dienst **25**(2): 9–99.

Becker, S., Hilgers, C., Kukla, P.A. & Urai, J.L., 2011. Crack-seal microstructure evolution in bi-mineralic quartz–chlorite veins in shales and siltstones from the RWTH-1 well, Aachen, Germany. Journal of Structural Geology **33**(4): 676–689. DOI: 10.1016/j.jsg.2011.01.001

Bentley, M. & Smith, S., 2008. Scenario-based reservoir modelling: the need for more determinism and less anchoring. *In*: T. Coussy & W.A. Muggeridge (Eds.), The future of geological modelling in hydrocarbon development (pp. 29–37, 1–309). London: Geological Society, Special Publications.

Bevandić, S., Blannin, R., Vander Auwera, J., Delmelle, N., Caterina, D., Nguyen, F. & Muchez, P., 2020. Geochemical and mineralogical characterisation of historic Zn–Pb mine waste, Plombières, East Belgium. Minerals **11**(1): 28. DOI: 10.3390/min11010028

Bless M.J.M., 1973. The history of the Finefrau Nebenbank Marine Band (Lower Westphalian A) in South Limburg (The Netherlands). Mededelingen Rijks Geologische Dienst **24**: 57–103.

Bless, M.J., Bouckaert, J. & Paproth, E., 1981b. Visé-Puth: Stimulant for further exploration? Annales de la Société géologique de Belgique **104**: 291–296.

Bless, M.J.M., Boonen, P., Bouckaert, J., Brauckmann, C., Conil, R., Dusar, M., Felder, P.J., Felder, W.M., Gökdag, H., Kockel, F., Laloux, M., Langguth, H.R., van der Meer Mohr, C.G., Meessen, J.P.M.T., op het Veld, F., Paproth, E., Pietzner, H., Plum, J., Poty, E., Scherp, A., Schultz, R., Streel, M., Thorez, J., van Rooijen, P., Vanguestaine, M., Vieslet, J.L., Wiesrma, D.J., Winkler Prins, C.F. & Wold, M., 1981a. Preliminary report on Lower Tertiary-Upper Cretaceous and Dinantian- Famennian rocks in the boreholes Heugem-1/la and Kastanjelaan-2 (Maastricht, The Netherlands). Mededelingen-Rijks Geologische Dienst **35**(15): 333–341.

Bless, M.J.M., Bosum, W., Bouckaert, J., Dürbaum, H.J., Kockel, F. & Paproth, E., 1980b. Geophysikalische Untersuchungen am Ost Rand des Brabanter Massivs in Belgien, den Niederlanden und der Bundesrepublik Deutschland. Mededelingen-Rijks Geologische Dienst **32**(17): 1–30.

Bless, M.J.M., Bouckaert, J., Bouzet, P., Conil, R., Cornet, P., Fairon-Demaret, M., Groessens, E., Longerstay, P.J., Meessen, J.T., Paproth, E. & Pirlet, H., 1976. Dinantian rocks in the subsurface North of the Brabant and Ardenno-Rhenish Massifs in Belgium, the Netherlands and the Federal Republic of Germany. Mededelingen-Rijks Geologische Dienst **27**(3): 81–195.

Bless, M.J.M., Bouckaert, J., Conil, R., Groessens, E., Kasig, W., Paproth, E., Poty, E., Van Steenwinkel, M., Streel, M. & Walter, R., 1980. Pre-Permian depositional environments around the Brabant Massif in Belgium, the Netherlands and Germany. Sedimentary Geology **27**(1): 1–81. DOI: 10.1016/0037-0738(80)90031-7

Bless, M.J.M., Bouckaert, J., Conil, R., Groessens, E., Kasig, W., Paproth, E., Poty, E., Van Steenwinkel, M., Streel, M. & Walter, R., 1980a. Pre-Permian depositional environments around the Brabant Massif in Belgium, the Netherlands and Germany. Sedimentary Geology **27**(1): 1–81. DOI: 10.1016/0037-0738(80)90031-7

Branchesi, M., Maggiore, M., Alonso, D., Badger, C., Banerjee, B., Beirnaert, F., Belgacem, E., Bhagwat, S., Boileau, G., Borhanian, S. & Brown, D.D., 2023. Science with the Einstein Telescope: a comparison of different designs. Journal of Cosmology and Astroparticle Physics **2023**(7): 68. DOI: 10.1088/1475-7516/2023/07/068

Brisson, S., Wellmann, F., Chudalla, N., von Harten, J. & von Hagke, C., 2023. Estimating uncertainties in 3-D models of complex fold-and-thrust belts: a case study of the Eastern Alps triangle zone. Applied Computing and Geosciences **18**: 100115. DOI: 10.1016/j.acags.2023.100115

Bulmer, M.G., 2012. Principles of statistics. Courier Corporation. New York, NY: Dover Publications, Inc.

Bultynck, P. & Dejonghe, L., 2002. Devonian lithostratigraphic units (Belgium). Geologica Belgica **4**(1–2): 39–69. DOI: 10.20341/gb.2014.043

Burchartz, R., Waldvogel, M., Chudalla, N., Achtziger-Zupančič, P., Wannenmacher, H., Vink, B., Linde, F., Orban, P., Spychala, Y., Hamdi, P. & Jalali, M., 2025. Einstein- Telescope in the Euregio-Meuse-Rhine–preliminary engineering geological site characterization for siting and design. Bulletin of Engineering Geology and the Environment **84**(12): 609. DOI: 10.1007/s10064-025-04623-2

Burs, D., Bruckmann, J. & Rüde, T.R., 2016. Developing a structural and conceptual model of a tectonically limited karst aquifer: a hydrogeological study of the Hastenrather Graben near Aachen, Germany. Environmental Earth Sciences **75**: 1–21. DOI: 10.1007/s12665-016-6039-x

Burt, A.K., Sirles, P. & Turner, A.K., 2021. Data sources for building geological models. *In*: A.K. Turner, H. Kessler & M.J. van der Meulen (Eds.), Geological modelling: applied geology and geophysics for engineers (1st ed.) (pp. 133–182). Hoboken, NJ: Wiley.

Caine, J.S., Evans, J.P. & Forster, C.B., 1996. Fault zone architecture and permeability structure. Geology **24**(11): 1025–1028. DOI: 10.1130/0091-7613(1996)024%3C1025:FZAAPS%3E2.3.CO;2

Chamberlin, T.C., 1965. The method of multiple working hypotheses: with this method the dangers of parental affection for a favorite theory can be circumvented. Science **148**(3671): 754–759. DOI: 10.1126/science.148.3671.754

Chaudoir, H., Lambert, L., Pastiels, A. & Willière, Y., 1953. Etude géologique du Bassin Houiller de Liège: les concessions Cheratte et Argenteau-Trembleur. Association pour l'Étude de la Paléontologie et de la Stratigraphie Houillères **17**: 1–109.

Clayton, G., Coquel, R., Doubinger, J., Gueinn, K.J., Loboziak, S., Owens, B. & Streel, M., 1977. Carboniferous miospores of Western Europe: illustration and zonation. Mededelingen-Rijks Geologische Dienst **29**: 1–71.

Coen-Aubert, M. & Boulvain, F., 2006. Frasnian. Geologica Belgica **9**: 1–2.

Cohen, K.M., Harper, D.A.T., Gibbard, P.L. & Car, N., 2023. ICS International Chronostratigraphic Chart 2023/09. International Commission on Stratigraphy. https://stratigraphy.org/ICSchart/ChronostratChart2023-09.pdf

Conil, R., 1964. Localités et coupes types pour l'étude du Tournaisien inférieur. Mémoires de l'Académie Royale de Belgique, Classe des Sciences. Collection Géologique **15**(4): 1–87.

Cuenca, M.C., Hooper, A.J. & Hanssen, R.F., 2013. Surface deformation induced by water influx in the abandoned coal mines in Limburg, The Netherlands observed by satellite radar interferometry. Journal of Applied Geophysics **88**: 1–11. DOI: 10.1016/j.jappgeo.2012.10.003

Databank Ondergrond Vlaanderen (DOV), 2025. Databank Ondergrond Vlaanderen. https://www.dov.vlaanderen.be

Davydov, V.I., Korn, D.K., Schmitz, M.D., Gradstein, F.M. & Hammer, Ø., 2012. The carboniferous period. *In*: F.M. Gradstein, J.G. Ogg, M.D. Schmitz & G.M. Ogg (Eds.), The Geologic Time Scale 2012 (pp. 603–651). Oxford/Amsterdam: Elsevier.

De la Varga, M. & Wellmann, J.F., 2016. Structural geologic modeling as an inference problem: a Bayesian perspective. Interpretation **4**(3): 1–16. DOI: 10.1190/INT-2015-0188.1

Dejonghe, L., 1998. Zinc–lead deposits of Belgium. Ore Geology Reviews **12**(5): 329–354. DOI: 10.1016/S0169-1368(98)00007-9

Delmer, A. & Graulich, J.M., 1959. Solution de quelques problèmes de stratigraphie houillère par la découverte de niveaux à goniatites. Bull. Soc. belge Géol **67:** 425–453.

Denayer, J., Prestianni, C., Mottequin, B., Hance, L. & Poty, E., 2021. The Devonian– Carboniferous boundary in Belgium and surrounding areas. Palaeobiodiversity and Palaeoenvironments **101**(2): 313–356. DOI: 10.1007/s12549-020-00440-5

Dikkers, A.J., 1945. De geologie van het veld van staatsmijn Maurits. Doctoral dissertation, van Aelst, Mededeelingen van de Geologische Stichting Serie C **I-1**(1): 1–88.

Dorsman, L., 1945. The marine fauna of the Carboniferous in the Netherlands (No. 3). Ernest van Aelst. Mededelingen van de Geologische Stichting Serie C **IV**(3-3): 1–101.

Esri Inc. ArcMap (version 2.6). Software, 2016. World Topographic map [basemap]. Scale Not Given. 'World Topographic' November 19, 2022. Redlands, CA: Esri Inc.

Everaerts, M. & De Vos, W., 2012. Gravity acquisition in Belgium and the resulting Bouguer anomaly map. Memoirs of the Geological Survey of Belgium, No. 58. Brussels: Geological Survey of Belgium.

Flude, S., Bond, C.E. & Butler, R.W., 2025. Are geological description practices and classification schemes fit for future use? Breccias as an example. Earth-Science Reviews **266:** 105140. DOI: 10.1016/j.earscirev.2025.105140

Fossen, H., 2016. Structural geology. Cambridge: Cambridge University Press.

Funtowicz, S.O. & Ravetz, J.R., 1990. Uncertainty and quality in science for policy (Vol. 15). Dordrecht: Springer Science & Business Media.

Geluk, M.C., Duin, E.T., Dusar, M., Rijkers, R.H.B., Van den Berg, M.W. & Van Rooijen, P., 1995. Stratigraphy and tectonics of the Roer Valley Graben. Geologie en Mijnbouw **73**: 129–129.

Geobasis NRW, 2025. Geobasisdaten der Kommunen und des Landes NRW. Krefeld: Geologischer Dienst NRW.

Geologisch Bureau, 1922. Boorrapport Baneheide (DB-115). Rijks Geologisch Bureau. Rapport GB 2072. Heerlen.

Geologisch Bureau, 1937. Boorrapport Mezzel-6 (DB-141). Rapport. Rijks Geologisch Bureau. Heerlen.

Graulich, J.M., 1955. La Faille eifélienne et le Massif de Herve: ses relations avec le Bassin houiller de Liège (pp. 1–31). Mémoire n° 1. Brussels: Service géologique de Belgique, Mémoires pour servir à l'explication des cartes géologiques et minières de la Belgique.

Geologisch Bureau, 1952. Rapport betreffende gegevens over het Carboon van de SM boringen LXVI, LXVII en LXVIII met stratigraphische gegevens uit het omliggende gebied. Rijks Geolisch Bureau. Rapport GB0550. Heerlen.

Geologisch Bureau, 1954. Over de mogelijkheden van exploratie van lood en zinkertsen in Zuid-Limburg. Rijks Geolisch Bureau. Rapport GB 0588. Heerlen.

Geologisch Bureau, 1985. Koolpetrografische analyses van de boringen GB 111, 113 en 115 (Zuid-Limburg) – Rijks Geolisch Bureau. Rapport GB 2072. Heerlen.

Gradstein, F.M. & Ogg, J.G., 2020. The chronostratigraphic scale. *In*: F.M. Gradstein, J.G. Ogg, M.D. Schmitz & G.M. Ogg (Eds.), Geologic time scale 2020 (pp. 21–32). Amsterdam: Elsevier.

Haites, T.B., 1948. Gelijkstelling der lagen in de mijngebieden van Zuid-Limburg en Aken en het bekken van Luik. Geologische Stichting (No. 2). Serie C-11-1. Heerlen.

Hance, L., Dejonghe, L., Ghysel, P., Laloux, M. & Mansy, J.L., 1999. Influence of heterogeneous lithostructural layering on orogenic deformation in the Variscan Front Zone (eastern Belgium). Tectonophysics **309**(1–4): 161–177. DOI: 10.1016/S0040-1951(99)00137-7

Hellemond, A., Van Uytfanghe, S., Van Wolterbeek, T. & Stein, K., 2019. De Famenniaanflora van Moresnet: Een vergeten paleobotanische locatie binnen een bijzonder geologisch en historisch kader. Spirifer **43**: 1–24.

Herbs, G., 1948. Schichten-verzeichnis der Bohrung Horbach VI. Geol. Landesamt Düsseldorf. Internal document. Krefeld.

Horion, C. & Gosselet, J., 1892. Etude stratigraphique sur les calcaires de Visé. Annales de la Société Géologique du Nord **20**: 194–212. DOI: 10.3406/asgn.1892.8876

Høyer, A.S., Sandersen, P.B.E., Andersen, L.T., Madsen, R.B., Mortensen, M.H. & Møller, I., 2024. Evaluating the chain of uncertainties in the 3D geological modelling workflow. Engineering Geology **343**: 107792. DOI: 10.1016/j.enggeo.2024.107792

Humblet, M., 1941. Le Bassin Houiller de Liége. Revue Universelle des Mines, 8e série, Tome XVII, no. 12. Liège.

Interreg EMR, n.d. E-test. https://www.interregemr.eu/projects/e-test

Jongmans, W.J. & Gothan, W., 1937. Betrachtungen über die Ergebnisse des Zweiten Kongresses für Karbonstratigraphie. *In*: Compte Rendu 2e Congrès International de Stratigraphie et de Géologie du Carbonifère, 1935 (Vol. 1, pp. 1–40). Heerlen.

Jongmans, W.J. & Robert, K., 1917. Flora of the carboniferous of the Netherlands and adjacent regions (Vol. 1, no. 7). Mededeelingen van de Rijksopsporing van Delfstoffen. 's Gravenhage.

Jongmans, W.J., 1928. Congrès pour l'étude de la stratigraphie du Carbonifère dans les différents centres houillers de l'Europe. *In*: Compte Rendu Congrès pour l'avancement des études de Stratigraphie Carbonifère, 1927 (pp. V–XLVIII). Heerlen.

Jongmans, W.J., Delepine, G., Gothan, W., Pruvost, P., Van Rummelen, F.H. & de Voogd, N., 1925. Geologische en paleontologische beschrijving van het Karboon der omgeving van Epen (Limb.). Natuurhistorisch Maandblad **14**(5): 55–83.

Joo, T., Chung, U. & Seo, M.G., 2020. Being Bayesian about categorical probability. *In*: Proceedings of the 37th International Conference on Machine Learning (ICML), PMLR, 13–18 July 2020 (pp. 4950–4961). Vienna.

Kasig, W., 1980. Dinantian carbonates in the Aachen region, Federal Republic of Germany. Mededelingen Rijks Geolische Dienst Nederland **32**: 44–52.

Kimpe, W.F.M., 1963. Geochimie des eaux dans le houiller du Limbourg (Pays-Bas). Verhandelingen Koninklijk Nederlands Geologisch Mijnbouwkundig Genootschap, Geologie Serie **21**: 25–45.

Kimpe, W.F.M., Bless, M.J.M., Bouckaert, J., Conil, R., Groessens, E., Meessen, J.T., Poty, E., Streel, M., Thorez, J. & Vanguestaine, M., 1978. Paleozoic deposits East of the Brabant Massif in Belgium and The Netherlands. Mededelingen-Rijks Geologische Dienst **30**(2): 37–103.

Kramer, G.J., Arts, T., Urai, J.L., Vrijling, H. & Huynen, J.M., 2020. Risk mitigation and investability of a U-PHS project in the Netherlands. Energies **13**(19): 5072. DOI: 10.3390/en13195072

Laloux, M., Geukens, F., Ghysel, P., Hance, L. & Servais, T., 2000. Gemmenich – Botzelaar, Henri-Chapelle-Raeren, Petergensfeld- Lammersdorf. Ministère de la Région Wallonne (95 p.). Namur: DGRNE.

Lambrecht, L., 1966. La stratigraphie du Namurien et du Westphalien inférieur dans la région de Dalhem-Mortroux. Annales de la Société géologique de Belgique **89**: 241–279.

Langenaeker, V., 2000. The Campine Basin. Stratigraphy, structural geology, coalification and hydrocarbon potential for the Devonian to Jurassic. Aardkundige Mededelingen (Leuven University Press) **10**: 142 pp + 4 maps.

Legrand, R., 1977. Précision sur le rejet de la Faille Bordière: Le sondage E4 bis à Villers- Saint-Siméon. Service géologique de Belgique. Professional Papers 9: 1–22, Bruxelles (Serv. géol. Belgique).

Lemon, A.M. & Jones, N.L., 2003. Building solid models from boreholes and user-defined cross-sections. Computers & Geosciences **29**(5): 547–555. DOI: 10.1016/S0098-3004(03)00051-7

Liu, L.L. & Wang, Y., 2022. Quantification of stratigraphic boundary uncertainty from limited boreholes and its effect on slope stability analysis. Engineering Geology **306**: 106770. DOI: 10.1016/j.enggeo.2022.106770

Ma, X., Fox, P., Rozell, E., West, P. & Zednik, S., 2014. Ontology dynamics in a data life cycle: challenges and recommendations from a geoscience perspective. Journal of Earth Science **25**: 407–412. DOI: 10.1007/s12583-014-0408-8

Mann, C.J., Davis, J.C. & Herzfeld, U.C., 1993. Uncertainty in geology. Computers in Geology **20**: 241–254.

MAPS for Europe, n.d. EURO-DEM dataset. https://www.mapsforeurope.org/datasets/euro-dem

Marshall, J.E., Reeves, E.J., Bennett, C.E., Davies, S.J., Kearsey, T.I., Millward, D., Smithson, T.R. & Browne, M.A., 2018. Reinterpreting the age of the uppermost 'Old Red Sandstone' and early carboniferous in Scotland. Earth and Environmental Science Transactions of the Royal Society of Edinburgh **109**(1–2): 265–278. DOI: 10.1017/S1755691018000968

Mascarelli, A.L., 2009. Quaternary geologists win timescale vote. Nature **459**: 624. DOI: 10.1038/459624a

Maurenbrecher, A.L.F.J., 1944. Kolenpetrographische studiën. Meded Geological Stitch Series C **III**(2): 1–108. Heerlen.

Maziane, N., Higgs, K.T. & Streel, M., 1999. Revision of the late Famennian miospore zonation scheme in eastern Belgium. Journal of Micropalaeontolgy **18**(1): 17–25. DOI: 10.1144/jm.18.1.17

Mijnlieff, H.F., 2020. Introduction to the geothermal play and reservoir geology of the Netherlands. Netherlands Journal of Geosciences **99**: e2. DOI: 10.1017/njg.2020.2

Mottequin, B., Denayer, J., Delcambre, B., Marion, J.M. & Poty, E., 2024. Upper Devonian lithostratigraphy of Belgium. Geologica Belgica **27**(3–4): 193–270. DOI: 10.20341/gb.2024.010

Mozafari, M., Gutteridge, P., Riva, A., Geel, K., Garland, J. & Dewit, J., 2019. Facies analysis and diagenetic evolution of the Dinantian carbonates in the Dutch subsurface. SCAN Programme (Seismische Campagne Aardwarmte Nederland).

Nitecki, M.H., Lemke, J.L., Pullman, H.W. & Johnson, M.E., 1978. Acceptance of plate tectonic theory by geologists. Geology **6**(11): 661–664. DOI: 10.1130/0091-7613(1978)6%3C661:AOPTTB%3E2.0.CO;2

NLOG, 2025. Netherland oil and gas portal. www.nlog.nl

Nyhuis, C.J., Riley, D. & Kalasinska, A., 2016. Thin section petrography and chemostratigraphy: integrated evaluation of an upper Mississippian mudstone dominated succession from the southern Netherlands. Netherlands Journal of Geosciences **95**(1): 3–22. DOI: 10.1017/njg.2015.25

Oncken, O., Von Winterfeld, C. & Dittmar, U., 1999. Accretion of a rifted passive margin: the Late Paleozoic Rhenohercynian fold and thrust belt (Middle European Variscides). Tectonics **18**(1): 75–91. DOI: 10.1029/98TC02763

Patijn, R.J.H. & Kimpe, W.F.M., 1961. De kaart van het Carboonoppervlak, de profielen en de kaart van het dekterrein van het Zuid-Limburgs mijngebied en Staatsmijn Beatrix met omgeving. Mededelingen van de Geologische Stichting, Serie C **I-1**(4): 12. Heerlen.

Patijn, R.J.H., 1963a. Het Carboon in de ondergrond van Nederland en de oorsprong van het Massief van Brabant. Geologie & Mijnbouw **42**: 341–349.

Patijn, R.J.H., 1963b. Tektonik von Limburg und Umgebung. Verhandelingen Koninklijk Nederlands Geologisch en Mijnbouwkundig Genootschap. Geologische Serie **21**(2): 9–24.

Pechnig, R., 2005. Auswertung der bohrlochgeophysikalischen Messungen in der RWTH-1 – Möglichkeiten und Grenzen der Lithologierekonstruktion. RWTH Aachen University, E. ON Energy Research Center, Appl Geophys Geotherm Energy, Unpublished.

Pirlet, H., 1967. Mouvements épeirogéniques Dévono-Carbonifère dans la region de Visé; la carriere de 'La Folie'à Bombay. Annales de la Société Géologique de Belgique **90**: 103–117.

Plisnier, M., 1931. Observations sur la tectonique des terrains primaires de la rive droite de la Meuse à Visé. Annales de la Société géologique de Belgique **LIV**: 207–213.

Polson, D. & Curtis, A., 2010. Dynamics of uncertainty in geological interpretation. Journal of the Geological Society **167**(1): 5–10. DOI: 10.1144/0016-76492009-055

Poty, E. & Delculée, S., 2011. Interaction between eustacy and block-faulting in the Carboniferous of the Visé-Maastricht area (Belgium, The Netherlands). Zeitschrift der Deutschen Gesellschaft für Geowissenschaften **162**(2): 117–126. DOI: 10.1127/1860-1804/2011/0162-0117

Poty, E., 1991. Tectonique de blocs dans le prolongement oriental du massif du Brabant. Annales de la Société Géologique de Belgique **114**(1): 265–275.

Pyrcz, M.J. & Deutsch, C.V., 2014. Geostatistical reservoir modeling (2nd ed.). New York, NY: Oxford University Press.

Raucq, P., 1942. La tectonique du Houiller dans les régions de Dalhem et de Val-Dieu. Annales de la Société Géologique de Belgique **65**: 70–85.

Reid, R.J. & Cowan, E.J., 2023. Towards quantifying uncertainties in geological models for mineral resource estimation through outside-in deposit-scale structural geological analysis. Australian Journal of Earth Sciences **70**(7): 990–1009. DOI: 10.1080/08120099.2023.2217882

Ribbert, K.H., 2006. Die Bohrung RWTH-1 – Regionalstratigraphische Einordnung und Deutung. Geologischer Dienst Nordrhein-Westfalen, vorläufiger Bericht, Internal Report. Aachen.

Rijks Geologische Dienst, 1995. Kaart subcrop Paleozoicum. Haarlem: Rijks Geologische Dienst. (Uit kaartserie van 4).

Sax, H.G., 1946. De tektoniek van het Carboon in het Zuid Limburgsch Mijngebied. Mededelingen van de Geologische Stichting Serie C **I-1**(3): 1–77.

Schweizer, D., Blum, P. & Butscher, C., 2017. Uncertainty assessment in 3-D geological models of increasing complexity. Solid Earth **8**(2): 515–530. DOI: 10.5194/se-8-515-2017

Sindern, S., Meyer, F.M., Lögering, M.J., Kolb, J., Vennemann, T. & Schwarzbauer, J., 2012. Fluid evolution at the Variscan front in the vicinity of the Aachen thrust. International Journal of Earth Sciences **101**(1): 87–108. DOI: 10.1007/s00531-011-0662-2

Sindern, S., Warnsloh, J.M., Trautwein-Bruns, U., Chatziliadou, M., Becker, S., Yuceer, S., Hilgers, C. & Kramm, U., 2008. Geochemical composition of sedimentary rocks and imprint of hydrothermal fluid flow at the Variscan front-an example from the RWTH-1 well (Germany). Zeitschrift der Deutschen Gesellschaft fur Geowissenschaften **159**(4): 623. DOI: 10.1127/1860-1804/2008/0159-0623

Sougnez, N. & Vanacker, V., 2011. The topographic signature of Quaternary tectonic uplift in the Ardennes massif (Western Europe). Hydrology and Earth System Sciences **15**(4): 1095–1107. DOI: 10.5194/hess-15-1095-2011

Sperrevik, S., Gillespie, P.A., Fisher, Q.J., Halvorsen, T. & Knipe, R.J., 2002. Empirical estimation of fault rock properties. *In*: Norwegian petroleum society special publications (Vol. 11, pp. 109–125). Elsevier, Amsterdam.

Stockmans, F., 1948. Végétaux du Dévonien Supérieur de la Belgique: Mémoires du Musée Royal d'histoire Naturelle de Belgique (Vol. 110, pp. 1–85). Brussels.

Streel, M., Higgs, K., Loboziak, S., Riegel, W. & Steemans, P., 1987. Spore stratigraphy and correlation with faunas and floras in the type marine Devonian of the Ardenne-Rhenish regions. Review of Palaeobotany and Palynology **50**(3): 211–229. DOI: 10.1016/0034-6667(87)90001-7

Thiadens, A.A., 1948. De Kampgroeve en de Kwartsietgroeve bij Cottessen in het Geuldal. Grondboor & Hamer **2**(4): 96–104.

Thorez, J., Streel, M., Bouckaert, J. & Bless, M.J.M., 1977. Stratigraphie et paléogéographie de la partie orientale du Synclinorium de Dinant (Belgique) au Famennien Supérieur: un modèle de bassin sédimentaire reconstitué par analyse pluridisciplinaire sédimentologique et micropaléontologique. Mededelingen-Rijks Geologische Dienst **28**(2): 17–32.

TNO-GDN, 2025a. Formatie van Zeeland. *In*: Stratigrafische Nomenclator van Nederland, TNO – Geologische Dienst Nederland. https://www.dinoloket.nl/stratigrafische-nomenclator/formatie-van-zeeland

TNO-GDN, 2025b. Formatie van Baarlo. *In*: Stratigrafische Nomenclator van Nederland, TNO – Geologische Dienst Nederland. https://www.dinoloket.nl/stratigrafische-nomenclator/formatie-van-baarlo

TNO-GDN, 2025c. Formatie van Epen. *In*: Stratigrafische Nomenclator van Nederland, TNO – Geologische Dienst Nederland. http://www.dinoloket.nl/stratigrafische-nomenclator/formatie-van-epen

TNO-GDN, 2025d. Limburg Group. *In:* Stratigrafische Nomenclator van Nederland, TNO – Geologische Dienst Nederland.

Torabi, A. & Berg, S.S., 2011. Scaling of fault attributes: a review. Marine and Petroleum Geology **28**(8): 1444–1460. DOI: 10.1016/j.marpetgeo.2011.04.003

Torabi, A., Ellingsen, T.S.S., Johannessen, M.U., Alaei, B., Rotevatn, A. & Chiarella, D., 2020. Fault zone architecture and its scaling laws: where does the damage zone start and stop? Geological Society **496**(1): 99–124. DOI: 10.1144/SP496-2018-151

Trautwein-Bruns, U., Hilgers, C., Becker, S., Urai, J.L. & Kukla, P.A., 2011. Fracture and fault systems characterising the intersection between the Lower Rhine Embayment and the Ardennes-Rhenish Massif – results from the RWTH-1 well, Aachen, Germany. Zeitschrift der Deutschen Gesellschaft fur Geowissenschaften **162**(3): 251–276. DOI: 10.1127/1860-1804/2011/0162-0251

Trautwein-Bruns, U., Schulze, K.C., Becker, S., Kukla, P.A. & Urai, J.L., 2010. In situ stress variations at the Variscan deformation front – results from the deep Aachen geothermal well. Tectonophysics **493**(1–2): 196–211. DOI: 10.1016/j.tecto.2010.08.003

Turner, A.K., Kessler, H. & van der Meulen, M.J. (Eds.), 2021. Applied multidimensional geological modeling: informing sustainable human interactions with the shallow subsurface. John Wiley & Sons, Hoboken.

Tversky, A. & Kahneman, D., 1973. Availability: a heuristic for judging frequency and probability. Cognitive Psychology **5**(2): 207–232. DOI: 10.1016/0010-0285(73)90033-9

Tversky, A. & Kahneman, D., 1974. Judgment under Uncertainty: Heuristics and Biases: Biases in judgments reveal some heuristics of thinking under uncertainty. Science **185**(4157): 1124–1131. DOI: 10.1126/science.185.4157.1124

Van Adrichem Boogaert, H.A. & Kouwe, W.F.P., 1994. Stratigraphic nomenclature of The Netherlands; revision and update by RGD and NOGEPA, Section B, Devonian and Dinantian. Mededelingen Rijks Geologische Dienst **50**: 1–20.

Van Waterschoot van der Gracht, W.A.J.M., 1909. The deeper geology of The Netherlands and adjacent regions with special reference to the latest borings in The Netherlands, Belgium and Westphalia, with contribution on the fossil flora by Dr W.J. Jongmans. Mededelingen van de Rijksopsporing van Delfstoffen **2**: 168–286.

Vis, G.J., Houben, A.J.P., Debacker, T.N. & Geel, C.R., 2025. The geological foundation of the Netherlands: the early Carboniferous, Devonian and older. *In*: J. Veen, G.J. Vis, J. Jager & T. Wong (Eds.), Geology of the Netherlands (pp. 21–93). Amsterdam: Amsterdam University Press.

Vis, G.J., Van Linden, E., Van Balen, R. & Cohen, K., 2020. Depressions caused by localized subsidence in the Netherlands, Belgium and Germany: a link with coal mining?. Proceedings of the International Association of Hydrological Sciences **382**: 201–205. DOI: 10.5194/piahs-382-201-2020

Wallonie, C., 2025. CIGALE platform. http://carto1.wallonie.be/CIGALE/viewer.htm?APPNAME=SSOL

Walter, R., 2010. Aachen und südliche umgebung: Nordeifel und nordost-Ardennen (Vol. 100). Stuttgart: Borntraeger.

Wei, W., Littke, R. & Swennen, R., 2023. Geochemical study of Mississippian to Pennsylvanian Namurian Shale in the Namur Synclinorium and Campine Basin (Belgium and S-Netherlands): implication for paleo-redox reconstruction and organic matter characteristics. International Journal of Coal Geology **265**: 104150. DOI: 10.1016/j.coal.2022.104150

WellCAD, 2022. WellCAD Version 5.7 [Computer software]. Windsor: Altair Engineering, Inc. https://www.alt.lu

Wellmann, J.F., Horowitz, F.G., Schill, E. & Regenauer-Lieb, K., 2010. Towards incorporating uncertainty of structural data in 3D geological inversion. Tectonophysics **490**(3–4): 141–151. DOI: 10.1016/j.tecto.2010.04.022

Wentworth, C.K., 1922. A scale of grade and class terms for clastic sediments. Journal of Geology **30**: 377–392. DOI: 10.1086/622910

Wood, B. & Kessler, H., 2021. Model creation based on digital borehole records and interpreted geological cross-sections. *In*: A.K. Turner, H. Kessler & M.J. van der Meulen (Eds.), Applied Multidimensional Geological Modeling: Informing Sustainable Human Interactions with the Shallow Subsurface (pp. 235–246). Hoboken, USA: Wiley-Blackwell.

Woodcock, N.H. & Mort, K., 2008. Classification of fault breccias and related fault rocks. Geological Magazine **145**(3): 435–440. DOI: 10.1017/S0016756808004883

Wrede, V. & Zeller, M., 1988. Geologie der Aachener Steinkohlenlagerstätte (Wurm- und Inde-Revier). Düsseldorf: Geologisches Landesamt Nordrhein-Westfalen.